# Biomass burning in Asia: annual and seasonal estimates and atmospheric emissions

D.G. Streets,[1*] K.F. Yarber,[1] J.-H. Woo,[2] and G.R. Carmichael[2]

[1]Decision and Information Sciences Division, Argonne National Laboratory, Argonne, IL

[2]Center for Global and Regional Environmental Research, University of Iowa, Iowa City, IA

Paper 2003GB002040

Submitted to *Global Biogeochemical Cycles*

Revised Manuscript, May 23, 2003

*Corresponding author: Tel: 630-252-3448; Fax: 630-252-5217; E-mail: dstreets@anl.gov

**Abstract.** A survey of biomass burning in Asia is developed to assist in the modeling of Asian and global air quality. A survey of national, regional, and international publications on biomass burning is conducted to yield consensus estimates of "typical" (i.e., non-year-specific) estimates of open burning (excluding biofuels). We conclude that 730 Tg of biomass are burned in a typical year from both anthropogenic and natural causes. Forest burning comprises 45% of the total, the burning of crop residues in the field comprises 34%, and 20% comes from the burning of grassland and savanna. China contributes 25% of the total, India 18%, Indonesia 13%, and Myanmar 8%. Regionally, forest burning in Southeast Asia dominates. National annual totals are converted to daily and monthly estimates at 1º × 1º grid resolution using distributions based on AVHRR fire counts for 1999-2000. Several adjustment schemes are applied to correct for the deficiencies of AVHRR data, including the use of moving averages, normalization, TOMS Aerosol Index, and masks for dust, clouds, landcover, and other fire sources. Good agreement between the national estimates of total burning and adjusted fire counts is obtained ($R^2$ = 0.71–0.78). Biomass burning amounts are converted to atmospheric emissions, yielding the following estimates: 0.37 Tg of $SO_2$, 2.8 Tg of $NO_x$, 1100 Tg of $CO_2$, 67 Tg of CO, 3.1 Tg of $CH_4$, 12 Tg of NMVOC, 0.45 Tg of BC, 3.3 Tg of OC, and 0.92 Tg of $NH_3$. Uncertainties in the emission estimates, measured as 95% confidence intervals, range from a low of ±65% for $CO_2$ emissions in Japan to a high of ±700% for BC emissions in India.

*INDEX TERMS:* 0322 Constituent sources and sinks; 0345 Pollution—urban and regional; 0365 Troposphere—composition and chemistry; 9320 Asia

## 1. Introduction

Biomass burning in Asia is an important contributor to air pollution in the region. We cannot hope to understand the measured concentrations of some of the key species around the Asian continent—particularly CO, particles, and $NO_x$—without allowing for emissions from biomass burning. However, our knowledge of biomass burning is extremely limited. Few long-term surveys of burning practices have been undertaken, nor have emission factors been estimated in the field. When the extreme inter-annual and intra-annual variability of burning is taken into account, it is clear that the estimation of the contribution of biomass burning to regional emissions is exceedingly hard to quantify. This paper develops estimates of "typical" amounts of biomass burning in the countries of Asia for a recent time period. The inventory is intended to complement a similar database of other anthropogenic emissions (biofuel combustion, fossil-fuel combustion, and non-combustion) in Asia [*Streets et al.*, 2003]. In combination, these inventories are being used to drive atmospheric chemistry and transport models, the results of which are then compared with observations. This work is primarily intended to support three field campaigns conducted in 2001-2002: the NASA TRACE-P (Transport and Chemical Evolution over the Pacific) mission, NSF/NOAA ACE-Asia (the Asian Pacific Regional Aerosol Characterization Experiment), and the NOAA ITCT (Intercontinental Transport and Chemical Transformation) mission.

This paper documents the development of a three-part inventory concerning biomass burning in Asia. The first part (Section 2 of this paper) is the creation of a comprehensive database detailing annual burning activity in Asia. The burning is divided into three activity types: forest fires, savanna or grassland fires, and the burning of crop residues in the field. All data are calculated and presented at the country level, and, for China, at the provincial level, using national surveys whenever possible. In the second part (Section 3), the spatial and temporal distributions of biomass burning are presented in gridded form for all of Asia, using landcover and satellite data to distribute the national, annual activity levels within a GIS environment. In the third part (Section 4), the activity data are used to create emission estimates for nine pollutant species: $SO_2$, $NO_x$, $CO_2$, CO, $CH_4$, NMVOC, BC, OC, and $NH_3$. Section 5 discusses some applications of this inventory in interpretation of the recent TRACE-P field observations.

There are differences among research publications in the definitions used for “biomass burning.” For the purposes of this paper, savanna/grassland burning is defined as the sum of all burning of grasslands arising from prescribed burning, natural fires, and grassland conversion. Forest burning is likewise defined as all on-site burning of forest biomass through both natural fire and deliberate man-made fires for land clearing or other purposes. Due to limitations in the available data, a few exceptions to these two definitions occur on a country-by-country basis, and these exceptions are noted in the text. Without exception, crop residue burning is defined as any deliberate burning of agricultural residues that occurs on-site. No off-site burning or biofuel combustion is included in these estimates.

The biomass burning estimates are not for any specific year, but are intended to represent "typical" annual amounts of vegetation burned and are characteristic of burning in the mid-1990s. This is intentional but also necessary, because there is no single data repository that contains estimates for all countries and all types of burning for a single year; our inventory is assembled from data of different vintages. In a few cases, we use long-term averages of burning taken from survey data; in most cases, though, we use data for individual years that were known to be moderate either in terms of the amount of burning that occurred or in terms of the prevailing meteorological conditions (no prolonged periods of drought or rain). We acknowledge the very large inter-annual variability in biomass burning. The values presented here are intended to be used in non-year-specific studies, such as future or generic air quality or climate simulations. For specific historical time periods, other analytical approaches are recommended, including the use of satellite data to identify actual burning amounts and locations. Sub-annual burning, including the periodicity of crop burning in the fields before, during, or after harvest, is treated using satellite observations, as described in Section 3.

## 2. Development of an Activity Inventory for Biomass Burning

### 2.1. Methodology

An inventory of biomass burning in Asia is developed using a compilation of data from a wide variety of sources. The general method used is a bottom-up approach, creating burning estimates based on vegetation cover and burn activity data in each country or region. Burning estimates tend to vary widely among publication sources. A comprehensive search of available data was conducted including examination of the peer-reviewed literature, individual country communications to the IPCC, Global Fire Monitoring Center publications, FAO statistics, and government/institute reports from individual countries. Information from all sources was collated and compared, and then consensus data were selected for inclusion in this inventory or used as a basis for the derivation of new values. Much of the literature on biomass burning, however, concerns itself with extreme events, such as the 1997 Indonesian fires [*Levine*, 1999] and the 1987 fires in northern China and Siberia [*Cahoon et al*., 1994]; we took care *not* to include such estimates in our survey work, which is aimed at quantifying typical burning amounts. In this sense, our work is not truly a long-term average of fire events in Asia. With few exceptions, no data exist to develop such averages.

Data in the literature on biomass burning were found in three forms: land area burned, emissions resulting from burning, or mass of biomass burned. When the actual mass of biomass burned was available, those data could be transferred directly into our inventory. When the data were in the other two forms, they had to be converted using the methods outlined below.

*Area Data*

For deriving the quantity of biomass burned from an estimate of the area of land burned, the following equation was used:

$$M = A * D * E \qquad (1)$$

where, $M$ = mass of dry matter burned;

$A$ = area burned;

$D$ = dry matter density; and

$E$ = fractional burn efficiency.

For savanna/grassland burning, two possible dry matter (dm) densities were used, depending on geographic location. For tropical Asia, the value used was 4.9 t dm $ha^{-1}$ [*IPCC*, 1997]. For extratropical Asia, the value used was 8.0 t dm $ha^{-1}$ [based on *Lavoué* *et al*., 2000]. Likewise, fractional burn efficiency was dependent on geographical location of the grassland. The values used were 0.85 (tropical Asia) and 0.90 (extratropical Asia). These burn efficiencies were based on a combination of the approaches used by the *IPCC* [1997] and *Lavoué et al.* [2000].

For forest burning, dry matter densities were taken from the IPCC country communication guidelines [*IPCC*, 1997]. Values were specific to type of forest region (tropical, temperate, and boreal), rainfall/humidity (wet, moist, dry, and montane), and (specific to Asian tropics) whether the forest was on insular or continental Asia. Burn efficiency was 0.6 for all types of forest. This is consistent with other biomass burning studies [*Hao and Liu*, 1994; *Lavoué et al*., 2000].

*Emissions Data*

When emissions from biomass burning in a given country or region were available, they were converted into quantity of biomass burned by dividing them by an activity-specific emission factor from *Andreae and Merlet* [2001]. In some cases, however, specific reports included enough information on their own calculation techniques that they could be used to back-calculate the original quantities of biomass burned. When this was the case, their methods and emission factors were preferred.

**2.1.1. Grassland/savanna and forest burning.** The methods for calculating grassland/savanna and forest burning depended on the best data available for the given region. Most studies were specific to a given sub-region of Asia or a particular country. Consistency across the various parts of the continent was impossible to obtain, except to the extent that one study, *Hao and Liu* [1994], was used where it could be corroborated by other work or where it was the only data available.

*South and Southeast Asia*

Burning estimates for forest and grassland fires in South and Southeast Asia have been calculated in previous work by *Hao and Liu* [1994]. These data are considered to be reliable, though somewhat dated now. They were used as default values where no other estimates could be found. The amounts of biomass burned each year from savanna and forest fires were calculated by *Hao and Liu* [1994] by multiplying activity data (area of land cleared each year) by aboveground biomass density and burn fraction. Their results were then presented at a spatially and temporally distributed level on gridded maps. To use these data, the original monthly data presented at a resolution of 5° x 5° had to be re-allocated to each country based on relative size and location. Then an annual country value was back-calculated from the monthly data using their temporal distribution formula. Unfortunately for our purposes, the data in *Hao and Liu* [1994] are representative of burning in the mid-1970s, whereas our inventory is intended to be for a typical year in the mid-1990s. This can be a source of error in our inventory, because we are sure that burning practices have changed since the mid-1970s. However, this uncertainty may not be as large as it might seem, because we surmise that burning increased with increasing rural population until 1985-1990 and then started to decline due to better land-management practices and an awareness of the ecological damage caused by excessive vegetation burning. This belief is largely based on anecdotal information, however, because few long-term burning surveys have been conducted and the trends are in any case obscured by inter-annual variability.

Data from *Hao and Liu* [1994] were used in our inventory for the following South and Southeast Asian countries: for forest and savanna burning in Bangladesh, Bhutan, Brunei, Cambodia, India, Malaysia, Myanmar, Nepal, Pakistan, Singapore, Sri Lanka, and Thailand; for forest burning (only) in Indonesia and Laos; and for grassland burning (only) in the Philippines and Vietnam. In many cases we had corroborative data for more recent years that supported the values of *Hao and Liu* [1994]; in the interests of inter-regional consistency, however, we adopted the *Hao and Liu* [1994] values.

A second data source was the country communications to the IPCC [available at http://www10.giscafe.com/goto.php?http://www.grida.no/db/maps/collection/climate6/index.htm]. When these values represented a complete description of burning activity, they were considered to be more reliable than the general or dated sources (such as *Hao and Liu* [1994]), because they were compiled for an international body by the countries themselves, who may reasonably be assumed to have the best knowledge of local burning practices. These values were often incomplete, though, and so were seldom used in this paper for anything but comparison purposes, unless they could be corroborated by other sources. *Houghton and Ramakrishna* [1999] have pointed out some of the problems with countries' accounting of their carbon sources and sinks in their official communications to the IPCC.

Relevant values in the IPCC reports are non-$CO_2$ emission estimates for forest and grassland conversion (in the land use change and forestry section), and non-$CO_2$ emission estimates for prescribed burning of savannas (in the agriculture section). Only non-$CO_2$ emissions were considered, because the IPCC guidelines for $CO_2$ calculations subtract an estimate of $CO_2$ re-absorption through subsequent vegetation re-growth, and this is incompatible with the needs of an analysis simply of the burning component. Non-$CO_2$ emission estimates (such as $CH_4$ emissions) were therefore converted to mass of biomass burned using the calculation guideline worksheets supplied by the IPCC [*IPCC*, 1997]. Such biomass burning estimates are therefore reliable only to the extent that each country followed the IPCC guidelines in its own calculations.

For both savanna and forest burning, values reported at this level are incomplete for our purposes. Whereas this paper seeks to quantify *all* biomass burning (both from natural or accidental fires and deliberate burning), the IPCC guidelines indicate that only deliberate burning need be included in a country communication. We therefore supplemented these figures with additional data from other sources on natural forest fires when possible. This method was used in calculating our reported values for forest fires in Indonesia, Japan, and Laos, and for grassland burning in the Philippines.

For Indonesia, a special entry for $CO_2$ emissions from naturally occurring forest fires was available in the country communication. From this entry, the mass of dry matter burned could be calculated using the $CO_2$ emission factor from *Andreae and Merlet* [2001]. Biomass burning from forest and grassland conversion was back-calculated from non-$CO_2$ emissions and the IPCC calculation worksheet. Dry matter burned in natural forest fires was added to dry matter burned on-site in forest and grassland conversion to supply our final forest burning estimate. No burn efficiency fraction was applied because it was assumed to be implicit in the country communication data.

Emissions for Laos were calculated similarly to Indonesia, by supplementing burning from forest and grassland conversion with a value for natural forest fires from the Lao PDR Country Report for the Asian Disaster Reduction Center (available at http://www.adrc.or.jp/countryreport/LAO/LAOeng99/Lao%20PDR%2099.htm). To this natural burning estimate, a burn efficiency of 0.6 was applied.

For the Philippines, the value presented in our inventory was calculated from non-$CO_2$ emissions for prescribed savanna burning. No other source of data for natural or accidental grassland fires was available to supplement the prescribed burning total. Moreover, the Philippines grassland burning estimate in *Hao and Liu* [1994] is zero. Since it is clear from the country communication that some burning does indeed occur, the *Hao and Liu* estimate was replaced by the value derived from prescribed burning. This may not represent all grassland burning in the Philippines, but it is a more accurate estimate than previously available and is based on the country's own assessment.

For comparison, other Asian countries were examined, and non-natural forest and savanna burning estimates were calculated whenever the data were available in country communications. Later, these burning estimates were compared to our final estimates, and in all cases were less than or equal to our values for total burning. It is assumed that the remaining dry matter is from natural fires, which are not addressed in the country communications.

Similar to the IPCC country communications are the 11 country reports for the ALGAS project of the Asian Development Bank on greenhouse-gas control (available at http://www.adb.org/Documents/Reports/ALGAS/default.asp). These reports present biomass burning emission estimates in the same format as the IPCC reports, and were treated for this work using the same methodology. The values derived from ALGAS were used mostly for comparison purposes, except for the burning of agricultural residues in Vietnam, for which they were used as the primary source (available at http://ntweb03.asiandevbank.org/oes0019p.nsf/pages/VIET_ES).

A final source examined was the Food and Agriculture Organization publication, *The State of the World's Forests* [*FAO*, 1997]. This report provides a country-by-country summary of the annual change in forest cover between 1990 and 1995. For our purposes, we attributed all change to forest burning, although loss of forest actually has a variety of causes. We converted annual change into mass burned by multiplying the deforestation rate by biomass density [based on *IPPC*, 1997] and a 0.6 burn efficiency fraction. This result was then used as an upper bound on *total possible* forest burning in each country (i.e., if all forest loss were due to burning).

All countries examined in our study were represented in *FAO* [1997], and in most cases the other estimates we obtained fell below that upper bound. That was not the case, however, for forest burning in Vietnam, which we initially based on *Hao and Liu* [1994]. *Hao and Liu* [1994] estimate 40.8 Tg dm burned per year, whereas the upper bound based on the *FAO* [1997] data is 15.0 Tg dm per year. This lower number was more consistent with other studies, such as the value of 8.2 Tg dm reported for forest and grassland conversion in ALGAS (back-calculated following guidelines in *IPCC,* 1997). Since the value of 8.2 Tg in ALGAS is known to only represent a portion of all forest burning, the final value given in our inventory for Vietnam is the value derived from *FAO* [1997]. This estimate is one of the most uncertain in our compilation.

*East and Northeast Asia*

The United Nations Economic Commission for Europe (UN/ECE) publishes a series of country reports detailing forest fire news, often of significant fire outbreaks. Many of these International Forest Fire News publications were consulted for this project (available at http://www2.ruf.uni-freiburg.de/fireglobe/iffn/country/country.htm). In general, when forest fires are quantified in these publications, they are presented in units of area of land burned per year. For our purposes, these figures were converted to mass of dry matter burned using the methodology outlined earlier. This method was used as our primary source of data for forest burning in the Republic of Korea. For other countries, it was only used for comparison and corroboration purposes.

For the Republic of Korea, a five-year average of forest area burned (1987-1991) was gathered from the International Forest Fire News [*UN/ECE*, 1995]. Area burned was converted to mass of dry matter burned using a density of 213 t dm $ha^{-1}$ from the IPCC country communication worksheets for temperate broadleaf forests [*IPCC*, 1997], and a burn efficiency of 0.6 (based on the range of burn efficiencies in *Hao and Liu* [1994] and *Lavoué et al*. [2000]).

Reliable data for grassland burning in China are not available due to the remoteness of these ecosystems; however, statistics on grassland coverage by Chinese provinces is available [*National Research Council*, 1992]. We determined the area of grassland burned in China by assuming the same percentage of grassland burned each year as in Mongolia. This resulted in our multiplying China's coverage area by 0.0297, the quotient of area of grassland burned in Mongolia [*Lavoué et al.*, 2000] and total grassland coverage in Mongolia [*UN/ECE*, 1999]. Once the area burned by province was determined, we applied the formula presented earlier for converting area to mass of dry matter burned. The grassland coverage area was presented by the National Research Council in two categories: "usable" and "unusable" or "degraded" land. To the usable portion, we applied a biomass density of 8.0 t $ha^{-1}$ and a burn efficiency of 0.6 [*IPCC*, 1997 and *Lavoué et al*., 2000, consensus values]. For the unusable/degraded portion, the biomass density was decreased to 2.0 t $ha^{-1}$ [*IPCC*, 1997]. The total mass of dry matter burned is the sum of the usable and unusable/degraded grassland burned for each province.

It is possible that this method overestimates grassland burning in western China, because of differences in climate, vegetation, or soil moisture between Mongolia and the western provinces. However, it should be noted that in the analysis of satellite fire-count data that follows (Section 3), biomass burning in this part of Asia appears to be significantly under-estimated, especially for Xinjiang, Qinghai, and Xizang Provinces of China and Mongolia itself. Frankly, these grasslands are so remote and un-monitored that any estimates of the extent of burning should be considered speculative at present.

China forest-fire data are from *Wang et al.* [1996]. In their original paper, data are compiled for a 42-year period, 1950-1992. The figures presented in this paper are the annual averages for each province during this period. Based on work in their paper, an annual deforestation estimate (area) was multiplied by a province-specific biomass density. The resulting value was then multiplied by a burn efficiency of 0.6.

The value for forest burning in Japan was derived from Japan's country communication to the IPCC. Methane emissions from on-site burning of forest matter after forest and grassland conversion were used in conjunction with the IPCC calculation guidelines [*IPCC*, 1997] to back-calculate mass of dry matter burned in deliberate fires. No additional quantities were added to reflect other types of forest fires.

No definitive data are available for fires in the Democratic People's Republic of Korea. Our value is calculated from an estimate of 114,000 acres burned in 1997 (a very dry year) (available at http://www.uswaternews.com/archives/arcglobal/7norkor8.html).

This extreme year is converted to an average year using the ratio of average-to-maximum burning (0.1655) for neighboring Heilongjiang Province of China from *Wang et al.* [1996]. Vegetation burned is then calculated using the IPCC vegetation density [*IPPC*, 1997] and a 0.6 burn fraction.

Forest and grassland burning amounts for Mongolia were taken from *Lavoué et al*. [2000], who present estimates of area burned in Mongolia over a 37-year period (1960-1997). We took an annual average of these data and then converted the area burned to mass of dry matter. For savanna/grassland burning, we used a density of 8.0 t dm $ha^{-1}$ and a burn efficiency of 0.9. For forest fires, the density used was 63.5 t dm $ha^{-1}$ for mixed broadleaf/coniferous boreal forests [*IPCC*, 1997] and the burn efficiency was 0.6.

The forest area burned in Taiwan, China, was taken from a study by the Taiwan Forestry Institute (available at http://www.tfri.gov.tw/publish/72-7e.htm). The area burned was converted to mass of dry matter using a biomass density of 185 t dm $ha^{-1}$ appropriate for tropical continental Asia [*IPCC*, 1997] and a burn efficiency of 0.6. For certain countries, savanna/grassland burning was assumed to be nonexistent due to the nature of their vegetation coverage. For these countries—namely Japan, the Republic of Korea, DPRK, and Taiwan, China—zero values are assigned in the grassland burning category.

**2.1.2. Crop residue burning.** Crop residue burning was calculated based on total crop production using the following equation:

$$R = P * N * D * B * F \qquad (2)$$

where, $R$ = total mass of crop residue burned in the field

$P$ = crop production

$N$ = crop-specific production-to-residue ratio

$D$ = dry-matter-to-crop ratio

$B$ = the percentage of dry matter residues that are burned in the field

$F$ = the crop-specific burn efficiency ratio.

Provincial-level crop production data for China were taken from the *China Statistical Yearbook* [2000]. For all other countries, data were gathered from the FAO Statistical Database [*FAO*, 2001]. Crops included are corn, oil crops, rice, roots/tubers, soybeans, sugarcane, and wheat. These are similar to the crop types chosen by *Hao and Liu* [1994]. In combination, these crops are believed to cover all significant crop-residue burning. Crop-specific production-to-residue ratios are based on work by *Koopmans and Koppejan* [1997], *Lu* [1993], and *Strehler and Stützle* [1987]. The corresponding dry matter fractions are taken from *Koopmans and Koppejan* [1997]. The percentage of dry matter burned in the field is taken for South Asia from Indian experience (C. Venkataraman, Indian Institute of Technology, Bombay, personal communication, 2001) and from *Hao and Liu* [1994] for the rest of Asia. This component of the calculation is a large source of uncertainty and points to a need for surveys of farmers' burning practices in different parts of Asia. Crop-specific burn efficiency ratios are based on work by *Turn et al*. [1997]. A complete summary of parameter values used is provided in Table 1.

When more reliable country-specific data were available, we deviated from the methodology above. These exceptions are noted in Table 2. Other sources of data for crop residue burning were the individual country communications to the IPCC. When these data were available, they were considered more reliable than data estimated using the methodology outlined above. This is because the countries themselves compiled them, and it is assumed that these countries have better information on local burning practices. When emissions data from the burning of agricultural residues in the field were available at all in country communications, they were included as a subset of the agriculture section. To calculate dry matter burned from emissions data in the crop-residue burning section of the country communications, the IPCC worksheets could not be used. This was because it would first be necessary to know which types of crops were included in each country's study, and the relative production of each crop (information that is not available). Therefore, for the purposes of this inventory, emissions data were converted to mass of dry matter burned using emission factors from *Andreae and Merlet* [2001]. This was used as our source of crop residue burning data for Japan, Indonesia, Malaysia, the Philippines, and Sri Lanka.

## 2.2. National Estimates of Biomass Burning

The resulting estimates of typical annual amounts of biomass burned in each Asian country can be found in Table 2 and Figure 1. It can be seen that many estimates come from *Hao and Liu* [1994]. This is because we found that their values agreed well with many of the other estimates we found in national and international statistics, and their use provided an additional element of consistency across the continent; where we preferred an alternative value or method, that is duly noted in Table 2. Table 3 presents similar information for each province of China. Figure 2 summarizes the information for four major regions of Asia. We estimate that 730 Tg of biomass are burned in Asia in a typical year, comprising 330 Tg of forest (45%), 250 Tg of crop residue (34%), and 150 Tg of grassland (20%). Our findings indicate that the greatest amount of biomass burning occurs in Southeast Asia (Figure 2), where 330 Tg of biomass are estimated to be burned in an average year. This is in great part because of the large amount of slash-and-burn agriculture and timber harvesting that occurs there. China and South Asia follow with 180 and 170 Tg per year, respectively. Crop-residue burning dominates biomass burning in each of these two regions. Compared to other regions, our Other East Asia region contributes little to the total amount of biomass burned in Asia with 34 Tg burned in an average year, mostly Mongolian grassland. In this region, there are few forests to burn, and the burning of agricultural residues is largely banned.

For comparison purposes, we also show in Tables 2 and 3 the amounts of biofuel consumed [*Streets et al.*, 2003]. These are the quantities of fuelwood, agricultural residues, and dried animal waste that are gathered and burned, largely to provide cooking and space heating needs in residential stoves. Across the Asian continent, we estimate that 79% more biomass is used to generate energy than is burned in the open (1300 Tg vs. 730 Tg). In China, this percentage is much higher (154%), because little vegetative material is wasted; rather it is collected and used (460 Tg biofuel vs. 180 Tg biomass burned in the open).

There are some significant differences in the values we chose to use for regional biomass burning estimates and those of previous publications on the topic. For China, our values come from forest-fire data calculated for each of the 31 Chinese provinces by *Wang et al*. [1996]. These regional values yield an annual-average total for China of 25

Tg biomass burned in forest fires. This is lower than the estimate of 40.5 Tg in *Galanter et al.* [2000], after adjustment to conform to the regions in our study. *Galanter et al.* [2000] also calculated adjusted values for savanna fires in China to be 9.2 Tg and crop residue burning to be 65.4 Tg, considerably lower than the values we calculate. We speculate that these shortfalls are due to the fact that significant amounts of biomass burning are unreported.

Our values for forest and savanna burning in South and Southeast Asia are very close to the *Hao and Liu* [1994] regional estimations of 70 Tg savanna burned and 340 Tg forest biomass burned in “Tropical Asia” (combined South and Southeast Asia). This is not surprising, because we adopted their values for many countries. Our estimate for forest fires in Southeast Asia is similar to that of *Galanter et al.* [2000], but our estimate for savanna and grassland burning is higher than theirs. For Indonesia our value for savanna fires [based on *Hao and Liu,* 1994] is higher than the values listed in country communications for the IPCC and ALGAS. We assume that the additional grassland burning can be attributed to natural fires (not included in those other studies). Our value for forest burning, 68 Tg, based on combined values for prescribed and natural fires in the country communication to the IPCC, is slightly lower than *Hao and Liu* [1994] (76 Tg), and significantly lower than the total deforestation estimate given in FAO [1997]. This is reasonable since only a portion of deforestation is from biomass burning. Estimates for South Asia by *Galanter et al.* [2000] are higher than ours by slightly more than one-third. For India our estimates are similar to those reported by Reddy and Venkataraman for savanna fires [*Reddy and Venkataraman,* 2000], forest fires [*Reddy and Venkataraman,* 2002] and crop-residue burning (C. Venkataraman, Indian Institute of Technology, Bombay, personal communication, 2001). It seems to us that certain other estimates of biomass burning in South Asia (see Table 4) are unreasonably high (see *Prasad et al*. [2001]), such as the values of 342 Tg for India [*Ahuja*, 1991] and 624 Tg for India+ (South Asia) [*Olivier et al*., 1996]. Of all the regions in our study, India stands out as urgently in need of a comprehensive survey of biomass burning, due to the wide variation in published estimates.

## 3. Spatial and Seasonal Allocation of Biomass Burning

Biomass burning is different from anthropogenic fuel combustion in terms of its causes, locations, and timing. An annual estimate of burned vegetation cannot be allocated over time and space in the same way as fuel combustion. The burning of crop residues is strongly correlated with agricultural practices (harvesting cycles, types of crops, regulatory requirements, etc.). Grassland and forest fires can correlate with both natural causes (lightning, precipitation, temperature, etc.) and human causes (land clearing for agriculture or habitation, timber harvesting, etc.). Because many of these factors are impossible to ascertain in the developing world, satellite information can play an important role in detecting and analyzing fire behavior [*Duncan et al.*, 2003; *Heald et al*., 2003; *Woo et al*., 2003]. The spatial and temporal variation of biomass burning emissions for this work, therefore, is derived from satellite information. We allocate the annual-regional emission data to daily-gridded form using satellite fire count information, and then aggregate them into monthly, seasonal, and annual gridded emission fields.

We selected the two-year period of January 1999 to December 2000 for the allocation procedure, because these two years are the closest available data set to the intensive flight measurement campaigns (TRACE-P and ACE-Asia) that can help to verify our methodology. Also, these two years have been shown to be typical (not excessively dry or wet) in terms of the amounts of burning that occurred. *Duncan et al.* [2003] presented inter-annual and intra-annual variation of satellite-derived fire counts using a 22-year record of NASA Total Ozone Mapping Spectrometer (TOMS) Aerosol Index (AI) data (available at http://toms.gsfc.nasa.gov/aerosols/aerosols.html) and a 4-year record of Along Track Scanning Radiometer (ATSR) data (available at http://shark1.esrin.esa.it/ionia/FIRE/ATSR/). In contrast to the ENSO-induced droughts of 1997-1998, which greatly enhanced Asian biomass burning, 1999 and 2000 were shown by *Duncan et al.* [2003] to be rather typical; the only unusual aspects were slightly enhanced burning in India and slightly reduced burning in Indonesia, both in 1999.

In our work, NOAA Advanced Very High Resolution Radiometer (AVHRR) fire count data (World Fire Web, available at http://ptah.gvm.sai.jrc.it/wfw/) and TOMS AI data (available at http://toms.gsfc.nasa.gov/aerosols/aerosols.html) are used to provide daily spatial/temporal variability representative of the period, as described below. The AVHRR sensor on board the NOAA series of polar orbiting satellites provides full global daily coverage (1.1 km × 1.1 km to 2.4 km × 6.9 km resolution) in five visible and infrared channels, and can be used to detect active fires. The World Fire Web (WFW) uses AVHRR data to map active fire events using a special contextual algorithm. Additional information about our method of using AVHRR and WFW fire count data can be found elsewhere [*Woo et al.*, 2003; *Stroppiana et al.*, 2000]. Since AVHRR fire count images provided from WFW are a snapshot along the satellite track, the designated overlaps remain in the dataset (along the track and strip edges). Also, the WFW dataset has two major problems arising from incomplete availability of AVHRR information: cloud interference and satellite coverage.

To adjust for missing data due to cloud cover and satellite coverage, we apply a normalization factor to the fire count data [*Woo et al*., 2003], i.e.,

$$FC_{adj\_i,j} = FC_{i,j} \frac{DC_{\max}}{Sam_{i,j} - Cld_{i,j}} \cos(lat_j) \tag{3}$$

where, $FC_{adj\_i,j}$ = adjusted fire count (i-th day, j-th grid)

$FC_{i,j}$ = original fire count (i-th day, j-th grid);

$Sam_{i,j}$ = satellite coverage frequency (i-th day, j-th grid);

$Cld_{i,j}$ = cloud coverage frequency (i-th day, j-th grid);

$DC_{max}$ = maximum data count of each grid; and

$\cos(lat_j)$ = latitude adjuster for $DC_{max}$ (radians, j-th grid).

However this process does not account for no-data grid cells or for data error conditions. For example, if $Sam_{i,j} = Cld_{i,j}$ or $Sam_{i,j} - Cld_{i,j} \tilde{} 0$, $FC_{adj\_i,j}$ cannot be calculated. In this case, we apply lower and upper bounds to the adjusted fire count. In cases where $FC_{i,j} = 0$ and $Sam_{i,j} = 0$, we use three-day moving averages (only applied to zero fire-count cells), as follows:

$$FC_{mov\_i,j} = \frac{(FC_{adj\_i-1,j} + FC_{adj\_i+1,j})}{2} \quad \text{when, } FC_{adj\_i,j} \le 0 \tag{4}$$

where, $FC_{adj\_i-1,j}$ = adjusted fire count (i-1th day, j-th grid); and

$FC_{adj\_i+1,j}$ = adjusted fire count (i+1th day, j-th grid).

If there was trouble in the satellite on-board system or at the receiving station, or if clouds persisted for more than several days, the moving average scheme cannot improve the AVHRR fire count data. In this case we use TOMS-AI data as an additional information source. However, the TOMS-AI data must be used with caution because it detects all aerosols, including dust and man-made smoke. So we applied several masks to filter the TOMS-AI signal that may not be caused by biomass burning. These masks include: 1) the classification of cloud conditions with and without rain using National Center for Environmental Prediction (NCEP) daily precipitation fields; 2) landcover maps [*ORNL*, 1998] to remove dust interference; and 3) maps of anthropogenic smoke sources, including coal mine fires, oil wells, and gas drilling sites [*Podwysocki*, 2000; *Steinshouer et al.*, 1999]. Figure 3 illustrates the datasets that were used to set the mask grids.

Figure 3a shows the maximum number of consecutive days of fire occurrence within the two-year period. Xinjiang, Nei Mongol, Liaoning, and Hebei Provinces of China, as well as Mongolia, Southeast Asia and South Asia, show high continuous occurrence of fire. The cloudiness image for the same period (Figure 3c) shows that cloud interference of the AVHRR fire count was lower in South Asia and continental Southeast Asia during this period, whereas the interference was higher in the Southeast Asian island countries (Malaysia, Indonesia, and Philippines). Fires below clouds cannot be detected by any satellites. One might think there would be little chance of fire below cloud because of the relatively high chance of rain, higher humidity, and lower temperature. But it is also possible that in some situations there might be a higher chance of fire below cloud, since lightning is a particularly important cause of fire in the world's boreal forests. So, it is important to distinguish between cloud with rain and cloud without rain. The NCEP daily precipitation fields were used to distinguish cloud with rain from cloud without rain (Figure 3d). The southern parts of Cambodia, Vietnam, Indonesia, Malaysia, and Philippines show higher incidence of clouds with precipitation. So, we presumed that the regions with high cloudiness and low precipitable cloud would mean a higher chance of "no-detection" in the AVHRR fire count. In that case, TOMS AI information can help detect missing fire information from AVHRR. Figure 3b shows the same kind of information as Figure 3a but for TOMS Aerosol Index (AI). It shows high values of AI in Pakistan, Northwest India, and Xinjiang and Hebei Provinces of China that is not likely to be biomass burning, because the landcover is primarily desert or dry cropland. These non-fire AI values can be masked out by our landcover mask because all the landcover classes except for cropland, savanna/grassland, and forest were excluded from the procedure.

Because of the uncertain factors described above, allocation of emissions based on fire counts is imperfect at best. We tested our fire count adjustment methodologies using correlation analysis between the regional biomass burning estimates (from Section 2) and the sum of fire counts within each region. We further separated them into the three different burning types (burning of agricultural residue, savanna/grassland, and forest) using landcover classes. Because the spatial resolutions of the landcover and fire count data are very different ($0.008^o \times 0.008^o$ vs. $1^o \times 1^o$), a single landcover cell cannot effectively represent one fire-count cell, in most cases. Therefore, we developed a procedure to estimate the area fraction of landcover types within each $1^o \times 1^o$ grid cell using 30 sec × 30 sec grid cells. Using the estimated area fraction of the three landcover classes in each 1º × 1º grid cell, we split the fire count of each grid cell by the fractions and then aggregate all fire counts within each region by burning type. The regional biomass burning amounts by the three different burning types were then allocated using this equation:

$$FC_{ik} = \sum_{j=1}^{P} LC_{ij} FC_{j} \quad (5)$$

where, $FC_{ik}$ = the regional sum of fire counts of the i-th burning type (agricultural, grassland, and forest) in the k-th region;

$LC_{ij}$ = the area fraction of i-th landcover within grid j;

$FC_{j}$ = the fire count in the j-th grid; and

$P$ = the number of grids in the region.

The actual amount of biomass burned in a given grid cell will be influenced by many factors, such as the probability of fire occurrence over a long time period, the type of agricultural waste and regulations pertaining to the burning of it, accumulated biomass prior to burning, climatological variation, etc. It is not possible to account for most of these factors over a large geographical area because datasets other than landcover are not available with the necessary detail. Our approach, therefore, should be considered as an initial effort to characterize emissions from different types of burning at continental scale.

The correlations between regional biomass burning estimates and fire counts by burning types and by the three different adjustment schemes are shown in Figure 4. For this correlation we divided India into four sub-regions so as to make its area more compatible with the other regions. Over the two-year period, the moving average is the best method to adjust fire count without consideration of burning type (Figure 4, upper left) in terms of coefficient of determination ($R^2$). However the AI adjustment scheme is better for the slope. All three adjustment schemes show much better agreement than the original fire count (0.25 vs. 0.71–0.78). Forest burning (lower right) shows by far the best agreement for all four cases ($R^2$ = 0.78-0.90). This is the best dataset for three reasons: (a) fires are larger, longer-lasting, and more intense, making them easier to observe from space; (b) forested areas are better defined and less intermingled with human habitation and oil/gas exploration activities, which can produce confounding satellite responses; and (c) governments show more concern about tracking and reporting forest fires for reasons of safety, air pollution, and control of timber exploitation, making the biomass burned data more reliable. On the other hand, the datasets on crop burning and grassland burning are much less certain. Crop burning may be illegal, is certainly small and dispersed, and leads to a weaker AVHRR response; grassland burning occurs in remote regions that are mostly beyond the means and the interest of government to monitor. These uncertainties are reflected in the correlations. For croplands, the adjustment schemes lead to values of $R^2$ = 0.52-0.62, though in all three cases a great improvement over the raw data ($R^2$ = 0.26). For grasslands, all four schemes produce lower values of $R^2$ = 0.37-0.46.

It is possible that the grassland case may be further confounded by some differences in the landcover classification schemes used in the biomass burning estimations and the fire count adjustments. Figure 4, lower left, shows that there are a number of Southeast Asian countries—Cambodia, Indonesia, Laos, Thailand, and Vietnam—that have estimates of grassland burning but no fire counts assigned to grasslands. All these countries have a lot of forest burning. Some of the burning observed from space may be occurring in areas that fall in between conventional definitions of forest and grassland, e.g., light woodland. When we tested this hypothesis by transferring 90% of the grassland to forest land, the $R^2$ values for grassland improved. This suggests the need to define a greater number of vegetation types in future work.

Figure 5 shows an alternative comparison between biomass burning estimates and fire counts by region. The biomass burning estimates are the standard line (0), and the differences for regional fire counts for the original data and for each adjustment scheme are presented. The scale of Y-axis is dimensionless because the data are normalized by the following equation:

$$FC_{\mathrm{norm,k}} = \frac{FC_k - FC_{mean,k}}{FC_{std,k}} \qquad (6)$$

*where,* $FC_{norm,k}$ = normalized fire count (k-th region);

$FC_k$ = fire count by adjusted schemes (k-th region);

$FC_{mean,k}$ = mean value of fire counts (k-th region); and

$FC_{std,k}$ = standard deviation of fire counts (k-th region).

Values greater than zero mean that the fire count is higher than the estimated biomass burned amount, and values less than zero mean that the fire count is lower than the biomass burned amount. In general, the regional biomass burned amounts are well matched with the fire counts after adjustment. The fire counts tend to be lower in Laos, Malaysia, Thailand, Vietnam, and Bangladesh, but higher in Mongolia and the Xinjiang and Xizang Provinces of China. One possible reason for these disagreements may be fire density. Since the satellite pinpoints the location of fires in 1 km × 1 km grid cells, the number of fires generally reflects the intensity of the fires. However, the biomass in a given area can be different for the different vegetation types. The fires in Southeast Asia are more likely to be the burning of forests and agricultural residues, whereas in Mongolia, Xinjiang, and Xizang the fires are more likely to be grassland fires that have lower vegetation density. Another reason can be interferences. As shown in Figure 3, Laos, Malaysia, Thailand, and Vietnam have higher precipitation, but are lower in cloudiness and AI values and therefore have little chance to be increased by the fire-count adjustment schemes. In contrast to this, Mongolia and Xinjiang have good characteristics to be increased. However, the normalized fire count was decreased after adjustments, in comparison to the original values, because we applied several masks to exclude "non-biomass-burning" fire counts.

We paid special attention to the possibility of man-made fires like oil/gas well flares in several regions where exploration and extraction activities are well-known, such as Pakistan, Qinghai, and Xinjiang. As presented in Figure 6, the AVHRR satellite can detect these "non-biomass-burning" fires because their sensing algorithm is highly dependent on temperature. We masked any $1^o \times 1^o$ grid cells that are located near known oil/gas fields [*Steinshouer et al.*, 1999] and showed many consecutive days of fire counts. These grid cells are excluded because biomass burning seldom continues for more than one week in a given grid cell. By applying these masking procedures, the fire count shows better agreement with the biomass burned amount, as shown in Figure 5. Nevertheless, despite our adjustments to the raw fire count, anomalies persist for Xinjiang and Mongolia. These two regions may require more in-depth study to pinpoint the sources of the fires seen in the AVHRR data. Also, the entire region in Figure 6 is dry and dusty, which provides a severe test to our dust mask in the TOMS-AI adjustment case. Of all regions in our Asia domain, it is Xinjiang Province that stands out as by far the greatest unexplained anomaly.

## 4. Atmospheric Emissions

To calculate emissions from biomass burning, the mass of dry matter burned of each type (forest, savanna grassland, or crop residues) is multiplied by an appropriate emission factor from *Andreae and Merlet* [2001], using the equation:

$$E = M * F \tag{7}$$

*where,* $E$ = total emissions of the source type;

$M$ = mass of dry matter burned; and

$F$ = source-specific emission factor (see Table 5).

Table 6 shows that the emissions of biomass burning in Asia contribute 0.37 Tg of $SO_2$, 2.8 Tg of $NO_x$, 1100 Tg of $CO_2$, 67 Tg of CO, 3.1 Tg of $CH_4$, 12 Tg of NMVOC, 0.45 Tg of BC, 3.3 Tg of OC, and 0.92 Tg of $NH_3$. The majority of these emissions originate in Southeast Asia, a region responsible for about the same quantity of emissions as all the other regions combined (Table 7). For some species, biomass burning is a major contributor to total anthropogenic emissions, comprising 20-30% of the total. In Table 7, we show that this is true for four species in particular: OC (32%), CO (24%), NMVOC (23%), and BC (18%) [*Streets et al.*, 2003]. In contrast, biomass burning contributes little (<5%) to total emissions of $SO_2$, $CH_4$, and $NH_3$.

Estimates of the uncertainties in these emissions have been performed in the broader context of total anthropogenic emissions in Asia [*Streets et al*., 2003], where additional details of our uncertainty methodology can be found. We acknowledge that for some types of biomass burning in some countries very little is known, and our choices for this inventory in these cases rely heavily on inferences of activity levels from quite limited and uncertain statistical information and the use of emission factors that are few and often not obtained from field studies. The uncertainty in our estimates is obtained by combining the coefficients of variation (CV, or the standard deviation divided by the mean) of the activities and emission factors, each derived separately for the three types of burning, the 52 source regions, and the nine chemical species. We tried wherever possible to use harmonized data across different source types and regions, even though the reporting practices of countries are not always consistent and available.

Since there is no rigorous way to judge the accuracy of activity estimates, expert judgment was used, classified according to a ten-point scale of CV, which varied for each group of provinces or countries based on the amount of information available and its perceived statistical quality. For the CV of emission factors, the uncertainty estimates provided by *Andreae and Merlet* [2001] were used. We have assumed that the underlying emission factor measurements are normally distributed [*Suutari et al*., 2001], but a case can be made for a lognormal distribution of combustion emission measurements (T.C. Bond *et al*., manuscript in preparation, 2003).

Combining uncertainties requires assumptions about the dependence or independence of parameters. To combine multiplicative, independent random variables such as activities and emission factors, we used Goodman's formula for the product of variables. The relative 95% confidence intervals for emissions are calculated as 1.96 times CV. However, combining uncertainties across provinces within a country, for example, is more problematic. When uncertainties are independent they can be combined in quadrature; this can be done for different sectors such as industry, residential, agriculture, biomass burning, etc. However, since the same emission factors may be used to calculate the emissions from two provinces, for example, these uncertainties are not independent and should not be added in quadrature. The same is true of two different sources for which an identical emission factor is used. For biomass burning, then, uncertainties are added linearly when the same emission factor is used, and uncertainties in emissions from different provinces are also added linearly. These aggregated uncertainties are then independent of each other and are combined in quadrature.

Figure 7 shows the results for each species for seven prototypical Asian regions. Our general findings are that emissions are known least well in India and the rest of South Asia. Emissions are best known in Japan and the other East Asian countries. Emissions of gases are known better than particles. The overall uncertainty in emissions for all of Asia is as follows, ranked in increasing order of uncertainty and measured as 95% confidence intervals: ±250% ($CO_2$), ±280% ($SO_2$), ±280% ($CH_4$), ±290% ($NO_x$), ±290% (NMVOC), ±300% (CO), ±310% ($NH_3$), ±420% (OC), and ±450% (BC). So, for example, we are 95% confident that Asian emissions of $CO_2$ are within ±250% of the stated value. As the confidence intervals are usually greater than the mean, our presentation of relative confidence intervals > ±100% might suggest that the lower confidence interval is negative. However, the true confidence interval is not symmetric about the mean, because some of the underlying variables are lognormally distributed. A better interpretation of "±400%", for example, might be "within a factor of five", so that the confidence interval would be 20-500% of the mean given.

## 5. Discussion

Carbon monoxide is the species most widely studied in regional and global modeling of biomass burning emissions, and good agreement is obtained with another estimate of Asian CO emissions from this source. In a study of Asian outflow to the Pacific Ocean, *Bey et al*. [2001] used a value of 61 Tg CO $yr^{-1}$, in good agreement with our estimate of 67 Tg. However, for TRACE-P analysis, our CO emissions estimate for open vegetation burning in March 2001 is about 30% lower than is estimated by *Heald et al.* [2003]; the spatial distribution is similar, however, because both come from the same set of satellite data. The values of *Duncan et al.* [2003] for Asia are also higher than ours. Their method is a combination of satellite data analysis and inventory development, similar to ours. For Southeast Asia, including Indonesia and Malaysia, their estimate of CO emissions from biomass burning is 118 Tg. Their region includes an unspecified part of China, but even if we include all of China, we only estimate about 45 Tg. Emission factors are very similar. The inclusion of the large burning event of 1997-1998 will necessarily raise their long-term average above ours. Much of the literature on amounts of biomass burning in Asia, including *Galanter et al*. [2000], *Bey et al.* [2001], *Duncan et al.* [2003], and *Heald et al*. [2003], use variants of the same unpublished inventory developed by Logan and Yevich at Harvard University. This means (a) that they all generate similar estimates, and (b) it is impossible to discover the causes of differences with other researchers' estimates. Clearly, there are good reasons to try to resolve inventory discrepancies in the future. A study by *Schultz* [2002] estimated 105 Tg CO for all Asia for the period 1997-2000 from ATSR satellite data. This is closer to our value. Schultz scaled data from *Hao and Liu* [1994], which we believe is high in some regions of Asia, as we have shown earlier in this paper.

Typical monthly distributions of these biomass burning emissions have been computed from the daily satellite fire counts over the two-year period, using CO as an illustrative example. First, countries were grouped into five regions according to broad latitudinal bands. Figure 8 shows the definitions of these regions (upper) and the monthly CO emissions. Southeast Asia and South Asia are the highest biomass-burning regions. The peak emission season is spring for these two regions and for southern China as well. Central China, northern China, Mongolia, Korea, and Japan show peak values in summer, though their emission amounts are small. Southeast Asia also shows a smaller peak in the fall. Seasonal CO emission distributions are presented in Figure 9. This illustrates the strong seasonal variation of emission distribution and amounts. The emissions are highest in spring, when Southeast Asia, South Asia, and southern China exhibit a high degree of biomass burning. However, the relative importance of central China and the northern regions increases in summer. Fall shows low emission amounts, but the relative importance of the Southeast Asian island regions increases. This result is consistent with *Schultz* [2002] for burning allocation.

The annual CO emission distribution by different burning types is shown in Figure 10. The high agricultural residue burning regions are central and eastern China, India and several regions in Southeast Asia. The high grassland burning areas are in Mongolia, Northwest China, India, and Pakistan. Southeast Asia is the biggest contributor to forest burning; eastern and northern parts of India and far northeastern China (Heilongjiang Province) also show relatively high forest-burning emissions.

As part of the NASA TRACE-P program, good agreement between modeling and observations using this inventory was obtained for 3-D chemical transport modeling [*Carmichael et al*., 2003; *Tang et al*., 2003; *Zhang et al*., 2003], chemical mass balance modeling [*Woo et al*., 2003], and chemical ratio analysis [*Ma et al*., 2003]. More information on daily emissions for the TRACE-P period (March/April, 2001) using the same scheme as this paper is also available [*Woo et al*., 2003].

A good example of the use of our data can be drawn from the modeling study of *Zhang et al*. [2003]. Figure 11 shows both CMAQ and STEM modeling results for CO during two TRACE-P DC8 flights (#11 and 12), in comparison with the aircraft observations. In the CMAQ case, model runs were conducted using our anthropogenic inventory, with and without the biomass burning component that is documented here. In the upper frame of Figure 11, elevated CO concentrations were observed on March 17 at an altitude of 2 km near Hong Kong (A1) and at an altitude of 3-4 km south of Shikoku Island of Japan (A2). A strong signal characteristic of biomass burning was associated with the episode A2, and it can be seen that inclusion of biomass burning emissions (open triangles) in the model gives quite good agreement with observations (closed circles)—certainly much better than model forecasts without biomass burning emissions (open circles).

Similarly, a high CO spike (more than 500 ppbv) was observed on March 18 in the boundary layer in the Taiwan Strait (B1 in the lower frame of Figure 11). This was due to a combination of fuel combustion emissions in China and biomass burning.

Though the models do not readily capture the height of the peak—a common feature of TRACE-P modeling that may reflect the inability of the model resolution to capture narrow pollution plumes leaving the Chinese mainland—the model results with biomass burning are in good agreement with a portion of this episode, as is also the case with episode B3, which represents post-frontal boundary layer outflow that includes biomass burning emissions.

In conclusion, this dataset represents the first comprehensive overview of typical biomass burning amounts in Asia. We show the different source strengths for different geographical regions, for different vegetation types, and for different seasons of the year. Information derived from national surveys is compared with satellite observations under several adjustment schemes and shown to produce good agreement for most of the region. Persistent problem areas are noted as good targets for improved understanding of biomass burning in Asia. We need to (a) undertake surveys to better understand how, when, and where farmers burn crop residues in the field; (b) better characterize and monitor the burning of remote grasslands; (c) re-examine the apparently anomalous AVHRR satellite responses in western China, especially Xinjiang Province; (d) consider ways to distinguish satellite signatures from vegetation burning and other man-made fires like oil/gas flares and coal-mine fires; and (e) develop new ways to integrate signals from different satellites, while masking out confounding responses.

The annual atmospheric emissions associated with this burning are also calculated. It is hoped that the datasets arising from this work will be helpful to other global and regional modelers interested in simulating atmospheric conditions under generic (non-year-specific) conditions, such as historical or future time periods. The $1^{o} \times 1^{o}$ gridded emissions from Asian biomass burning described in this paper can be examined and downloaded from our TRACE-P emissions web site at the University of Iowa: http://www.cgrer.edu/EMISSION_DATA/index_16.htm.

**Acknowledgments.** This work was funded by the National Aeronautics and Space Administration under grant NCC-1-422 to the University of Iowa. The work at Argonne National Laboratory was supported by a sub-contract with the University of Iowa. Argonne National Laboratory is operated by the University of Chicago under Contract No. W-31-109-ENG-38 with the U.S. Department of Energy.

## References

Ahuja, D.R., Estimating regional anthropogenic emissions of greenhouse gases, in *Indian Geosphere Biosphere Programme: Some Aspects*, edited by T.N. Khoshoo and M. Sharma, pp. 131-162, Haranand Publications, New Delhi, 1991.

Andreae, M.O., and P. Merlet, Emissions of trace gases and aerosols from biomass burning, *Global Biogeochem. Cycles, 15,* 955-966, 2001.

Bey, I., D.J. Jacob, J.A. Logan, and R.M. Yantosca, Asian chemical outflow to the Pacific in spring: Origins, pathways, and budgets, *J. Geophys. Res.*, *106*, 23,097-23,113, 2001.

Cahoon, D.R., B.J. Stocks, J.S. Levine, W.R. Cofer, and J.M. Pierson, Satellite analysis of the severe 1987 forest fires in northern China and southeastern Siberia, *J. Geophys. Res.*, *99*, 18,627-18,638, 1994.

Carmichael, G.R., Y. Tang, G. Kurata, I. Uno, D.G. Streets, J.-H. Woo, H. Huang, J. Yienger, B. Lefer, R.E. Shetter, D.R. Blake, A. Fried, E. Apel, F. Eisele, C. Cantrell, M.A. Avery, J.D. Barrick, G.W. Sachse, W.L. Brune, S.T. Sandholm, Y. Kondo, H.B. Singh, R.W. Talbot, A. Bandy, A.D. Clarke, and B.G. Heikes, Regional-scale chemical transport modeling in support of intensive field experiments: overview and analysis of the TRACE-P observations, *J. Geophys. Res.*, in press, 2003.

*China Agricultural Yearbook*, China Agricultural Press, Beijing, 2000.

*China Statistical Yearbook*, China Statistical Publishing House, State Statistical Bureau, Beijing, 2000.

Duncan, B.N., R.V. Martin, A.C. Staudt, R. Yevitch, and J.A. Logan, Interannual and seasonal variability of biomass burning emissions constrained by satellite observations, *J. Geophys. Res.*, *108* (D2), 4040, doi:10.1029/2002JD002378, 2003.

FAO, FAOSTAT Agricultural Database, Food and Agriculture Organization, Rome, 2001 (available at http://apps.fao.org/page/collections?subset=agriculture).

FAO, *State of the World's Forests 1997*, Food and Agriculture Organization, Rome, 1997.

Galanter, M., H. Levy, and G.R. Carmichael, Impacts of biomass burning on tropospheric CO, $NO_x$, and $O_3$, *J. Geophys. Res.*, *105*, 6633-6653, 2000.

Hao, W.M., and M. Liu, Spatial and temporal distribution of tropical biomass burning, *Global Biogeochem. Cycles*, *8*, 495-503, 1994.

Heald, C.L., D.J. Jacob, P.I. Palmer, M.J. Evans, G.W. Sachse, H.B. Singh, and D.R. Blake, Biomass burning emission inventory with daily resolution: application to aircraft observations of Asian outflow, *J. Geophys. Res.*, in press, 2003.

Houghton, R.A., and K. Ramakrishna, A review of national emissions inventories from select non-annex I countries: implications for counting sources and sinks of carbon, *Annu. Rev. Energy Environ.*, *24*, 571-605, 1999.

Intergovernmental Panel on Climate Change (IPCC), *Greenhouse Gas Inventory Workbook: Revised 1996 IPCC Guidelines for National Greenhouse Gas Inventories*, vol.2, edited by J.T. Houghton, Bracknell, U.K., 1997.

Joshi, V., Biomass Burning in India, in *Global Biomass Burning: Atmospheric, Climatic, and Biospheric Implications*, edited by J.S. Levine, pp. 185-193, MIT Press, Cambridge, MA, 1991.

Koopmans, A., and J. Koppejan, Agricultural and forest fires: Generation, utilization and availability, paper presented at the Regional Consultation on Modern Applications of Biomass energy, Kuala Lumpur, Malaysia, 1997.

Lavoué, D., H. Cachier, J.G. Goldammer, C. Liousse, and B.J. Stocks, Modeling of carbonaceous particles emitted by boreal and temperate wildfires at northern latitudes. *J. Geophys. Res., 105*, 26,871-26,890, 2000.

Levine, J.S., The 1997 fires in Kalimantan and Sumatra, Indonesia: gaseous and particulate emissions, *Geophys. Res. Lett*., *26*, 815-818, 1999.

Lu, Y., *Fueling One Billion: An Insider's Story of Chinese Energy Policy Development*, Washington Institute Press, Washington D.C., 1993.

Ma, Y., R.J. Weber, Y.-N. Lee, D.A. Orsini, K. Maxwell-Meier, D.C. Thornton, A.R. Bandy, A.D. Clarke, D.R. Blake, G.W. Sachse, H.E. Fuelberg, C.M. Kiley, J.-H. Woo, D.G. Streets, and G.R. Carmichael, The characteristics and influence of bio-smoke on the fine particle ionic composition measured in Asian outflow during TRACE-P, *J. Geophys. Res.*, in press, 2003.

National Research Council, *Grasslands and Grassland Sciences in Northern China*, National Academy Press, Washington, DC, 1992.

Oak Ridge National Laboratory (ORNL), *LandScan Global Population 1998 Database*, Oak Ridge National Laboratory, Oak Ridge, TN, 1998.

Olivier, J.G.J., A.F. Bouwman, C.W.M. van der Maas, J.J.M. Berdowski, C. Veldt, J.P.J. Bloos, A.J.H. Visschedijk, P.Y.J. Zandveld, and J.L. Haverlag, Description of EDGAR Version 2.0, National Institute of Public Health and the Environment Report No. 771060 002, Bilthoven, The Netherlands, 1996.

Podwysocki, S., *Coal-Bearing Regions and Structural Sedimentary Basins of China and Adjacent Seas: Coal-bearing regions*, U.S. Geological Survey Open-File Report 00-047, USGS, Eastern Energy Resources Team, Reston, VA, 2000.

Prasad, V.K., Y. Kant, P.K. Gupta, C. Sharma, A.P. Mitra, and K.V.S. Badarinath, Biomass and combustion characteristics of secondary mixed deciduous forests in Eastern Ghats of India, *Atmos. Environ*., *35*, 3085-3095, 2001.

Reddy, M.S. and C. Venkataraman, Atmospheric optical and radiative effects of anthropogenic aerosol constituents from India. *Atmos. Environ., 34*, 4511-4523, 2000.

Reddy, M.S. and C. Venkataraman, Inventory of aerosol and sulphur dioxide emissions from India. Part II—biomass combustion, *Atmos. Environ., 36*, 699-712, 2002.

Schultz, M.G., On the use of ATSR fire count data to estimate the seasonal and interannual variability of vegetation fire emissions, *Atmos. Chem. Phys. Discuss*., *2*, 1159-1179, 2002.

Steinshouer, D.W., J. Qiang, P.J. McCabe, and R.T. Ryder, *Maps showing geology, oil and gas fields, and geologic provinces of the Asia Pacific Region*, U.S. Geological Survey Open-File Report 97-470F, U.S. Geological Survey, Denver, CO, 1999.

Streets, D.G., T.C. Bond, G.R. Carmichael, S. Fernandes, Q. Fu, D. He, Z. Klimont, S.M. Nelson, N.Y. Tsai, M.Q. Wang, J.-H. Woo, and K.F. Yarber, An inventory of gaseous and primary aerosol emissions in Asia in the year 2000, *J. Geophys. Res*., in press, 2003.

Strehler, A., and W. Stutzle, Biomass residues, in *Biomass*, edited by D.O. Hall and R.P. Overend, pp. 75-102, John Wiley and Sons, New York, 1987.

Stroppiana, D., S. Pinnock, and J.-M. Gregoire, The Global Fire Product: daily fire occurrence from April 1992 to December 1993 derived from NOAA AVHRR data, *Int. J. Remote Sensing, 21,* 1279-1288, 2000.

Suutari, R., M. Amann, J. Cofala, Z. Klimont, M. Posch, and W. Schopp, *From Economic Activities to Ecosystem Protection in Europe: An Uncertainty Analysis of Two Scenarios of the RAINS Integrated Assessment Model*, CIAM/CCE Report 1/2001, joint report of the International Institute for Applied Systems Analysis, Laxenburg, Austria, and the National Institute of Public Health and the Environment, Bilthoven, The Netherlands, 2001.

Tang, Y., G.R. Carmichael, J.-H. Woo, N. Thongboonchoo, G. Kurata, I. Uno, and D.G. Streets, The influences of biomass burning during the TRACE-P experiment identified by the Regional Chemical Transport Model, *J. Geophys. Res.*, in press, 2003.

Turn, S.Q., B.M. Jenkins, J.C. Chow, L.C. Pritchett, D. Campbell, T. Cahill, and S.A. Whalen, Elemental characterization of particulate matter emitted from biomass burning: Wind tunnel derived source profiles for herbaceous and wood fuels, *J. Geophys. Res.*, *102,* 3683-3700, 1997.

UN/ECE, Forest and Steppe Fire Monitoring in Mongolia Using Satellite Remote Sensing, *International Forest Fire News*, No. 21, United Nations Economic Commission for Europe, Geneva, 1999.

UN/ECE, Forest fires: Background, Statistics, Management and Research, *International Forest Fire News*, No. 13, United Nations Economic Commission for Europe, Geneva, 1995.

Wang, X., Z. Feng, and Y. Zhuang, Forest fires in China: carbon dioxide emissions to the atmosphere, in *Biomass Burning and Global Change*, vol.2, edited by J.S. Levine, pp.771-778, MIT Press, Cambridge, MA, 1996.

Woo, J.-H., D.G. Streets, G.R. Carmichael, Y. Tang, B. Yoo, W.-C. Lee, N. Thongboonchoo, S. Pinnock, G. Kurata, I. Uno, G.W. Sachse, D.R. Blake, A. Fried, and D.C. Thornton, The contribution of biomass and biofuel emissions to trace gas distributions in Asia during the TRACE-P experiment, *J. Geophys. Res*., in press, 2003.

Zhang, M., I. Uno, Z. Wang, H. Akimoto, G.R. Carmichael, Y. Tang, J.-H. Woo, D.G. Streets, G.W. Sachse, M.A. Avery, R.J. Weber, and R.W. Talbot, Large-scale structure of trace gas and aerosol distributions over the Western Pacific Ocean during TRACE-P, *J. Geophys. Res*., in press, 2003.

**Figure Captions**

**Figure 1.** Estimates of the amounts of vegetation burned annually, by country and biomass type.

**Figure 2.** Regional comparison of vegetation burned annually, by biomass type. Regions are China (not including Taiwan, China); Other East Asia (Japan; Republic of Korea; DPR Korea; Mongolia; and Taiwan, China); Southeast Asia (Brunei, Cambodia, Indonesia, Laos, Malaysia, Myanmar, Philippines, Singapore, Thailand, and Vietnam); and South Asia (Bangladesh, Bhutan, India, Nepal, Pakistan, and Sri Lanka).

**Figure 3.** Asian distributions of a) fire duration from AVHRR; b) aerosol index duration from TOMS; c) cloudiness; and d) precipitable cloud.

**Figure 4.** Correlations between regional biomass burning amounts and AVHRR fire counts in 1999-2000, by vegetation type (total, cropland, grassland, and forest), for the raw data (Original) and three different cumulative adjustment procedures (Normalized, Normalized + Moving Averaged, and Normalized + Moving Averaged + AI Adjusted).

**Figure 5.** Normalized differences between regional biomass burning amounts and AVHRR fire counts for the raw data (Original) and three different cumulative adjustment procedures (Normalized, Normalized + Moving Averaged, and Normalized + Moving Averaged + AI adjusted).

**Figure 6.** Superimposed AVHRR average fire counts at $1^{o} \times 1^{o}$ resolution and oil/gas field locations in western China, western Mongolia, and northern India and Pakistan.

**Figure 7.** Uncertainty (%) in emission estimates for seven prototypical Asian regions and nine pollutant species (±95% confidence intervals).

**Figure 8.** Definition of regions (upper) and monthly CO emissions (Gg) from biomass burning (lower).

**Figure 9.** Spatial distribution (1º × 1º resolution) of seasonal CO emissions (t $season^{-1}$ per grid cell) from biomass burning: a) winter, b) spring, c) summer, d) fall.

**Figure 10.** Spatial distribution (1º × 1º resolution) of annual CO emissions (t $yr^{-1}$ per grid cell) from biomass burning by vegetation type: a) agricultural residues, b) grassland, c) forest, d) total.

**Figure 11.** Time series of observed (closed circles, ppbv) and simulated [*Zhang et al*., 2003] concentrations of CO with (open triangles, ppbv) and without (open circles, ppbv) biomass burning emissions along the TRACE-P flight tracks (dashed line, altitude in km). Also shown are the corresponding STEM model calculated CO concentrations (solid line, ppbv) [*Carmichael et al*., 2003]. Flights are DC8 flights 11 (upper) and 12 (lower) on March 17 and 18, 2001, respectively. Flight segments A1, A2, B1, and B3 are discussed in the text. This figure is excerpted from *Zhang et al*., 2003.

**Table 1.** Parameters Used in the Calculation of Crop Residue Burning

| Type of Vegetation | Production-to-Residue Ratio[a] | Dry Matter Fraction[a] | Dry Matter Burned in the Field (%) | | Burn Efficiency[d] |
|---|---|---|---|---|---|
| | | | South Asia[b] | Rest of Asia[c] | |
| Corn | 2.0 | 0.40 | 25 | 17 | 0.92 |
| Oil crops | 0.6[e] | 0.85 | 25 | 17 | 0.82 |
| Rice | 1.76 | 0.85 | 25 | 17 | 0.89 |
| Roots/tubers | 0.2[e] | 0.71 | 25 | 17 | 0.68 |
| Soybeans | 0.21[f] | 0.71 | 25 | 17 | 0.68 |
| Sugarcane | 0.3 | 0.71 | 25 | 17 | 0.68 |
| Wheat | 1.75 | 0.83 | 25 | 17 | 0.86 |

[a] Unless noted otherwise, all values are from *Koopmans and Koppejan* [1997].
[b] C. Venkataraman, Indian Institute of Technology, Bombay, personal communication, 2001.
[c] *Hao and Liu* [1994].
[d] *Turn et al*. [1997].
[e] *Lu* [1993].
[f] *Strehler and Stützle* [1987].

**Table 2.** Typical Annual Amounts of Biomass Burned in Asian Countries, with Biofuel Use Included for Comparison

| Country | Grassland (Tg)[a] | Forest (Tg)[a] | Crop Residue (Tg)[b] | Total (Tg) | Biofuel Use (Tg)[c] |
|---|---|---|---|---|---|
| Bangladesh | 0.0 | 8.5 | 11 | 20 | 37 |
| Bhutan | 0.0 | 0.7 | 0.0 | 0.7 | 1.2 |
| Brunei | 0.0 | 0.0 | 0.0 | 0.0 | 0.1 |
| Cambodia | 7.6 | 5.4 | 0.9 | 14 | 6.4 |
| China | 52[d] | 25[e] | 110 | 180 | 460 |
| India | 8.6 | 37 | 84 | 130 | 420 |
| Indonesia | 21 | 68[f] | 5.8[g] | 95 | 140 |
| Japan | 0.0 | 0.6[f] | 1.9[g] | 2.4 | 3.9 |
| Korea, DPR | 0.0 | 1.0[h] | 0.9 | 1.8 | 18 |
| Korea, Rep. of | 0.0 | 0.1[i] | 1.7 | 1.8 | 1.1 |
| Laos | 4.9 | 19[j] | 0.5 | 25 | 2.2 |
| Malaysia | 0.0 | 22 | 0.8[g] | 23 | 5.5 |
| Mongolia | 23[k] | 9.2[k] | 0.0 | 33 | 1.8 |
| Myanmar | 1.9 | 56 | 4.0 | 61 | 22 |
| Nepal | 0.0 | 5.0 | 2.0 | 7.0 | 16 |
| Pakistan | 2.9 | 0.9 | 10 | 14 | 61 |
| Philippines | 0.2 | 17 | 7.1 | 24 | 16 |
| Singapore | 0.0 | 0.0 | 0.0 | 0.0 | 6.9 |
| Sri Lanka | 0.0 | 3.9 | 0.2 | 4.1 | 9.1 |
| Taiwan, China | 0.0 | 0.1[l] | 0.4 | 0.6 | 0.3 |
| Thailand | 12 | 36 | 7.7 | 56 | 19 |
| Vietnam | 12 | 15[m] | 6.1[n] | 33 | 57 |
| Asia Total | 150 | 330 | 250 | 730 | 1300 |

[a]Entries in columns not marked with a footnote are from *Hao and Liu* [1994].
[b]For the general method used for crop residues, see text; exceptions to this method are noted in additional footnotes below.
[c]Data are from *Streets et al.* [2003], including fuelwood, agricultural residues, and dried animal waste.
[d]The coverage area is from *National Research Council* [1992], converted to area burned using *UN/ECE* [1999] and *Lavoué et al.* [2000]. Area burned is converted to dry matter using *IPCC* [1997] and *Lavoué et al.* [2000].
[e]Values are from *Wang et al.* [1996].
[f]Calculated using data gathered for the country communication to the IPCC.
[g]Calculated using country communication to the IPCC and the emission factor from *Andreae and Merlet* [2001].
[h]Calculated from 1997 area burned (see text). This extreme year is converted to an average year using *Wang et al.* [1996]. Vegetation burned is calculated using IPCC vegetation density and burn fraction [*IPCC*, 1997].
[i]Area burned is from *UN/ECE* [1995], converted using *IPCC* [1997], *Hao and Liu* [1994], and *Lavoué et al.* [2000].
[j]Country communication to the IPCC back-calculated using *IPCC* [1997] and Lao PDR Country Report for ADRC (see text).
[k]Average annual area of savanna and forest burned from *Lavoué et al.* [2000]. Area is converted to dry matter burned using *Lavoué et al.* [2000] and *IPCC* [1997].
[l]Area burned estimated from a Taiwan study (see text), converted to biomass burned using *IPCC* [1997].
[m]Area calculated from *FAO* [1997], converted to dry matter using *IPCC* [1997].
[n]Emissions data from ALGAS study (see text), converted to dry matter using *IPCC* [1997].

**Table 3.** Typical Annual Amounts of Biomass Burned in the Provinces of China, with Biofuel Use Included for Comparison

| Province | Grassland (Tg)[a] | Forest (Tg)[b] | Crop Residue (Tg)[c] | Total (Tg) | Biofuel Use (Tg)[d] |
|---|---|---|---|---|---|
| Anhui | 0.0 | 0.1 | 6.5 | 6.6 | 17 |
| Beijing | 0.0 | 0.0 | 0.3 | 0.4 | 1.6 |
| Fujian | 0.0 | 0.6 | 2.0 | 2.6 | 12 |
| Gansu | 2.4 | 0.0 | 1.3 | 3.7 | 7.4 |
| Guangdong | 0.0 | 0.5 | 4.7 | 5.2 | 8.8 |
| Guangxi | 0.0 | 0.9 | 4.6 | 5.5 | 20 |
| Guizhou | 0.0 | 0.6 | 1.9 | 2.5 | 17 |
| Hainan | 0.0 | 0.0 | 0.5 | 0.5 | 1.1 |
| Hebei | 0.0 | 0.0 | 5.4 | 5.4 | 19 |
| Heilongjiang | 1.2 | 9.5 | 6.3 | 17 | 24 |
| Henan | 0.0 | 0.1 | 8.8 | 9.0 | 26 |
| Hong Kong | 0.0 | 0.0 | 0.0 | 0.0 | 0.0 |
| Hubei | 0.0 | 0.3 | 5.9 | 6.2 | 32 |
| Hunan | 0.0 | 0.3 | 6.3 | 6.5 | 29 |
| Jiangsu | 0.0 | 0.0 | 1.8 | 1.8 | 32 |
| Jiangxi | 0.0 | 0.3 | 8.0 | 8.3 | 20 |
| Jilin | 0.3 | 0.5 | 6.0 | 6.8 | 17 |
| Liaoning | 0.4 | 0.1 | 2.3 | 2.7 | 23 |
| Nei Mongol | 16 | 5.0 | 2.7 | 23 | 9.9 |
| Ningxia | 0.6 | 0.0 | 0.6 | 1.1 | 1.9 |
| Qinghai | 7.4 | 0.0 | 0.2 | 7.7 | 1.1 |
| Shaanxi | 0.0 | 0.1 | 2.3 | 2.5 | 11 |
| Shandong | 0.0 | 0.0 | 7.4 | 7.5 | 31 |
| Shanghai | 0.0 | 0.0 | 0.5 | 0.5 | 0.9 |
| Shanxi | 0.0 | 0.1 | 1.5 | 1.6 | 2.3 |
| Sichuan | 0.2 | 0.7 | 9.1 | 9.9 | 55 |
| Tianjin | 0.0 | 0.0 | 0.5 | 0.5 | 1.7 |
| Xinjiang | 11 | 0.1 | 0.6 | 11 | 3.9 |
| Xizang | 13 | 0.1 | 1.4 | 15 | 0.6 |
| Yunnan | 0.0 | 5.2 | 2.8 | 8.0 | 20 |
| Zhejiang | 0.0 | 0.1 | 3.3 | 3.3 | 18 |
| China Total | 52 | 25 | 110 | 180 | 460 |

[a]Values based on *IPCC* [1997], *UN/ECE* [1999], *Lavoué et al.* [2000], and *National Research Council* [1992] (see text).
[b]*Wang et al.* [1996].
[c]See text for the calculation method used.
[d]Data are from *Streets et al.* [2003], including fuelwood, agricultural residues, and dried animal waste.

**Table 4.** Comparison of Estimates of Biomass Burned (Tg) in India

| Country/ Region | Year | Vegetation Type: Savanna/ Grassland | Vegetation Type: Forest | Vegetation Type: Crop Residue | Total Vegetation Consumed | Reference |
|---|---|---|---|---|---|---|
| India | n/s | 24.8 | 103.3 | 214.0 | 342.1 | *Ahuja* [1991] |
| S. Asia | n/s | 21.1 | 84.5 | 156.6 | 262.2 | *Galanter et al*. [2000] |
| India | 1985/86 | | 102.6 | | | *Joshi* [1991] |
| India+ [a] | n/s | 95.0 | 113.2 | 82.0 | 290.2 | R. Yevich, Harvard University, personal communication, 2001. |
| India | 1990 | 5.2 | 26.7 | | | *Reddy and Venkataraman* [2000] |
| India+ [a] | 1990 | 10.8 | 75.8 | 537.0 | 623.6 | *Olivier et al*. [1996] |
| India | 1996/97 | | 39.0 | | | *Reddy and Venkataraman* [2002] |
| India | 1996/97 | | | 81.4 | | C. Venkataraman, Indian Institute of Technology, Bombay, personal communication, 2001. |
| India | "typical" | 8.6 | 37 | 84 | 130 | this work |
| S. Asia | “typical” | 11 | 57 | 110 | 180 | this work |

[a] India+ includes Bangladesh, Bhutan, India, Maldives, Myanmar, Nepal, Pakistan, and Sri Lanka.

n/s = not specified.

**Table 5.** Emission Factors for Biomass Burning (g $kg^{-1}$)

| Vegetation Type | $SO_2$ | $NO_x$ | NMVOC[a] | CO | BC | OC | $NH_3$ | $CO_2$ | $CH_4$ |
|---|---|---|---|---|---|---|---|---|---|
| Savanna/Grassland | 0.35 | 5.98 | 9.73 | 65 | 0.48 | 3.4 | 1.05 | 1613 | 2.3 |
| Tropical Forest | 0.57 | 2.45 | 19.32 | 104 | 0.66 | 5.2 | 1.3 | 1580 | 6.8 |
| Extratropical Forest | 1 | 4.6 | 21.79 | 107 | 0.56 | 9.15 | 1.4 | 1569 | 4.7 |
| Crop Residue | 0.4 | 3.83 | 15.7 | 92 | 0.69 | 3.3 | 1.3 | 1515 | 2.7 |

Source: *Andreae and Merlet* [2001].

[a] An emission factor for NMVOC was derived by combining the emission factors of many individual NMVOC species in *Andreae and Merlet* [2001].

**Table 6.** Total National Emissions from Biomass Burning in Asia (Gg)

| Country | $SO_2$ | $NO_x$ | $CO_2$ | CO | $CH_4$ | NMVOC | BC | OC | $NH_3$ |
|---|---|---|---|---|---|---|---|---|---|
| China | 83 | 820 | 280000 | 16000 | 540 | 2700 | 110 | 730 | 230 |
| Japan | 1.3 | 9.7 | 3700 | 230 | 7.6 | 41 | 1.6 | 11 | 3.2 |
| Korea, Rep. of | 0.8 | 7.0 | 2800 | 170 | 5.1 | 29 | 1.2 | 6.4 | 2.4 |
| Korea, DPR | 1.3 | 7.8 | 2800 | 180 | 6.9 | 35 | 1.1 | 12 | 2.5 |
| Mongolia | 17 | 180 | 52000 | 2500 | 97 | 430 | 16 | 160 | 38 |
| Taiwan, China | 0.2 | 1.9 | 840 | 52 | 2.0 | 9.1 | 0.4 | 2.1 | 0.7 |
| Brunei | 0.0 | 0.0 | 0 | 0 | 0.0 | 0 | 0.0 | 0.0 | 0.0 |
| Cambodia | 6.1 | 62 | 22000 | 1100 | 57 | 190 | 7.8 | 57 | 16 |
| Indonesia | 48 | 310 | 150000 | 9000 | 530 | 1600 | 59 | 440 | 120 |
| Laos | 13 | 78 | 39000 | 2400 | 140 | 420 | 15 | 120 | 31 |
| Malaysia | 13 | 57 | 36000 | 2400 | 150 | 440 | 15 | 120 | 30 |
| Myanmar | 34 | 160 | 97000 | 6300 | 390 | 1200 | 40 | 310 | 79 |
| Philippines | 12 | 69 | 37000 | 2400 | 130 | 440 | 16 | 110 | 31 |
| Singapore | 0.0 | 0.0 | 0 | 0 | 0.0 | 0 | 0.0 | 0.0 | 0.0 |
| Thailand | 28 | 190 | 88000 | 5200 | 290 | 930 | 35 | 250 | 69 |
| Vietnam | 15 | 130 | 53000 | 2900 | 150 | 500 | 20 | 140 | 40 |
| Bangladesh | 9.3 | 63 | 30000 | 1900 | 88 | 340 | 13 | 81 | 25 |
| Bhutan | 0.7 | 3.2 | 1100 | 75 | 3.3 | 15 | 0.4 | 6.3 | 1.0 |
| India | 74 | 540 | 200000 | 12000 | 420 | 2200 | 83 | 650 | 170 |
| Nepal | 5.8 | 31 | 11000 | 710 | 29 | 140 | 4.2 | 52 | 10 |
| Pakistan | 6.0 | 61 | 22000 | 1200 | 39 | 210 | 9.0 | 52 | 18 |
| Sri Lanka | 2.3 | 10 | 6500 | 430 | 27 | 79 | 2.7 | 21 | 5.4 |
| Asia Total | 370 | 2800 | 1100000 | 67000 | 3100 | 12000 | 450 | 3300 | 920 |

**Table 7.** Regional Emissions from Biomass Burning (Tg) and Share of Total Emissions

| Region | Emissions (Tg) | | | | | | | | |
|---|---|---|---|---|---|---|---|---|---|
| | $SO_2$ | $NO_x$ | $CO_2$ | CO | $CH_4$ | NMVOC | BC | OC | $NH_3$ |
| China | 0.08 | 0.82 | 280 | 16 | 0.54 | 2.7 | 0.11 | 0.73 | 0.23 |
| Other East Asia | 0.00 | 0.21 | 62 | 3.1 | 0.12 | 0.54 | 0.021 | 0.20 | 0.05 |
| Southeast Asia | 0.17 | 1.1 | 520 | 32 | 1.8 | 5.7 | 0.21 | 1.6 | 0.41 |
| *of which, Indonesia* | *0.05* | *0.31* | *150* | *9.0* | *0.53* | *1.6* | *0.059* | *0.44* | *0.12* |
| South Asia | 0.10 | 0.71 | 270 | 17 | 0.61 | 3.0 | 0.11 | 0.86 | 0.23 |
| *of which, India* | *0.07* | *0.54* | *200* | *12* | *0.42* | *2.2* | *0.083* | *0.65* | *0.17* |
| Asia total biomass burning | 0.37 | 2.8 | 1100 | 67 | 3.1 | 12 | 0.45 | 3.3 | 0.92 |
| Asia other emissions[a] | 34 | 25 | 8700 | 210 | 100 | 40 | 2.1 | 7.1 | 27 |
| Asia total emissions[b] | 34 | 27 | 9900 | 280 | 110 | 52 | 2.5 | 10 | 28 |
| Biomass burning share (%) | 1.1 | 11 | 12 | 24 | 2.9 | 23 | 18 | 32 | 3.3 |

[a] Emissions from energy, industry, and agriculture [*Streets et al*., 2003].
[b] Total anthropogenic emissions, including biomass burning but excluding natural sources such as volcanoes, biogenic NMVOC, and $CH_4$ from wetlands [*Streets et al*., 2003].

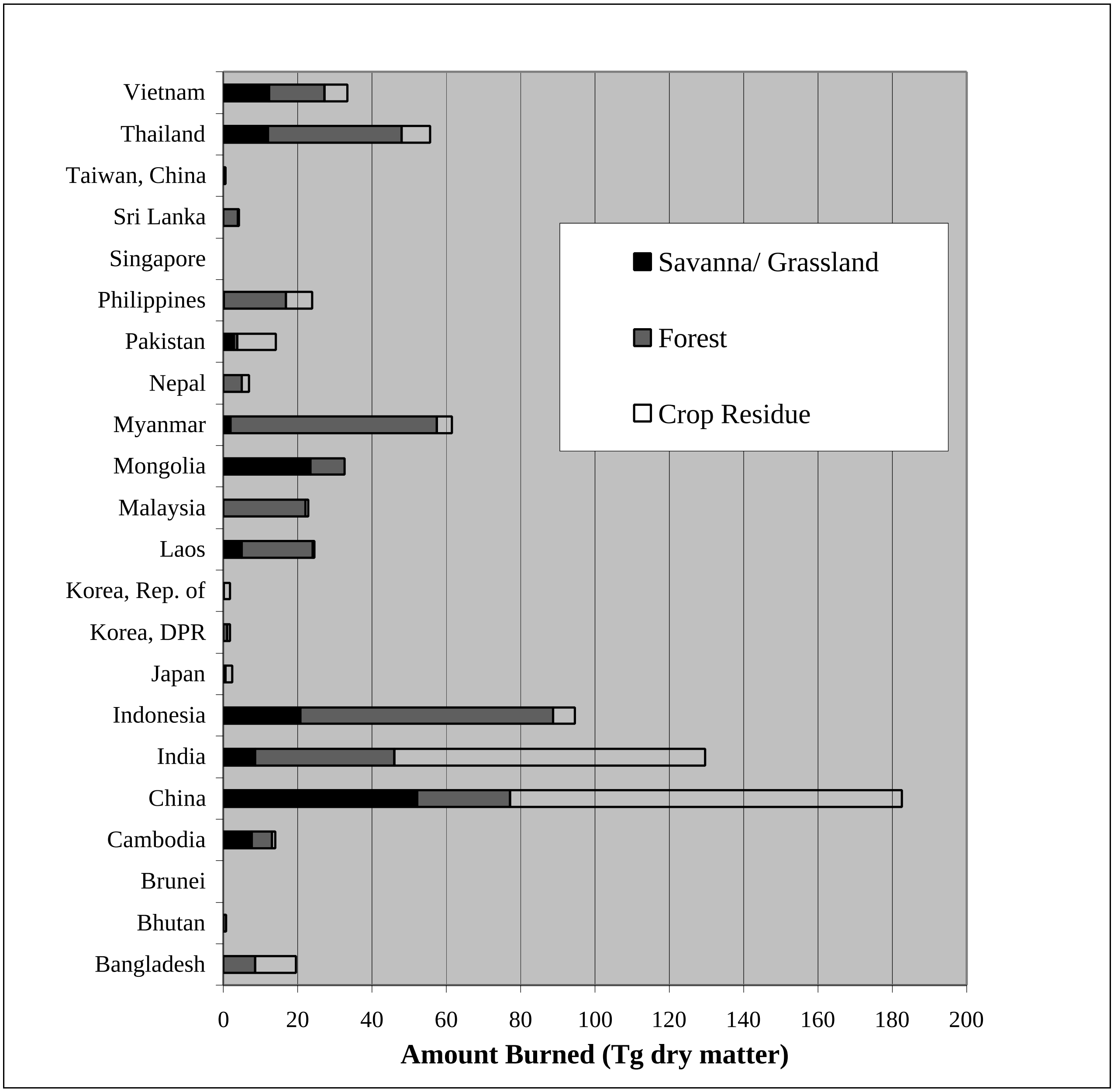
Vietnam
Thailand
Taiwan, China
Sri Lanka
Singapore
Philippines
Pakistan
Nepal
Myanmar
Mongolia
Malaysia
Laos
Korea, Rep. of
Korea, DPR
Japan
Indonesia
India
China
Cambodia
Brunei
Bhutan
Bangladesh
Savanna/ Grassland
Forest
Crop Residue
0
20
40
60
80
100
120
140
160
180
200
Amount Burned (Tg dry matter)

**Figure 1.**

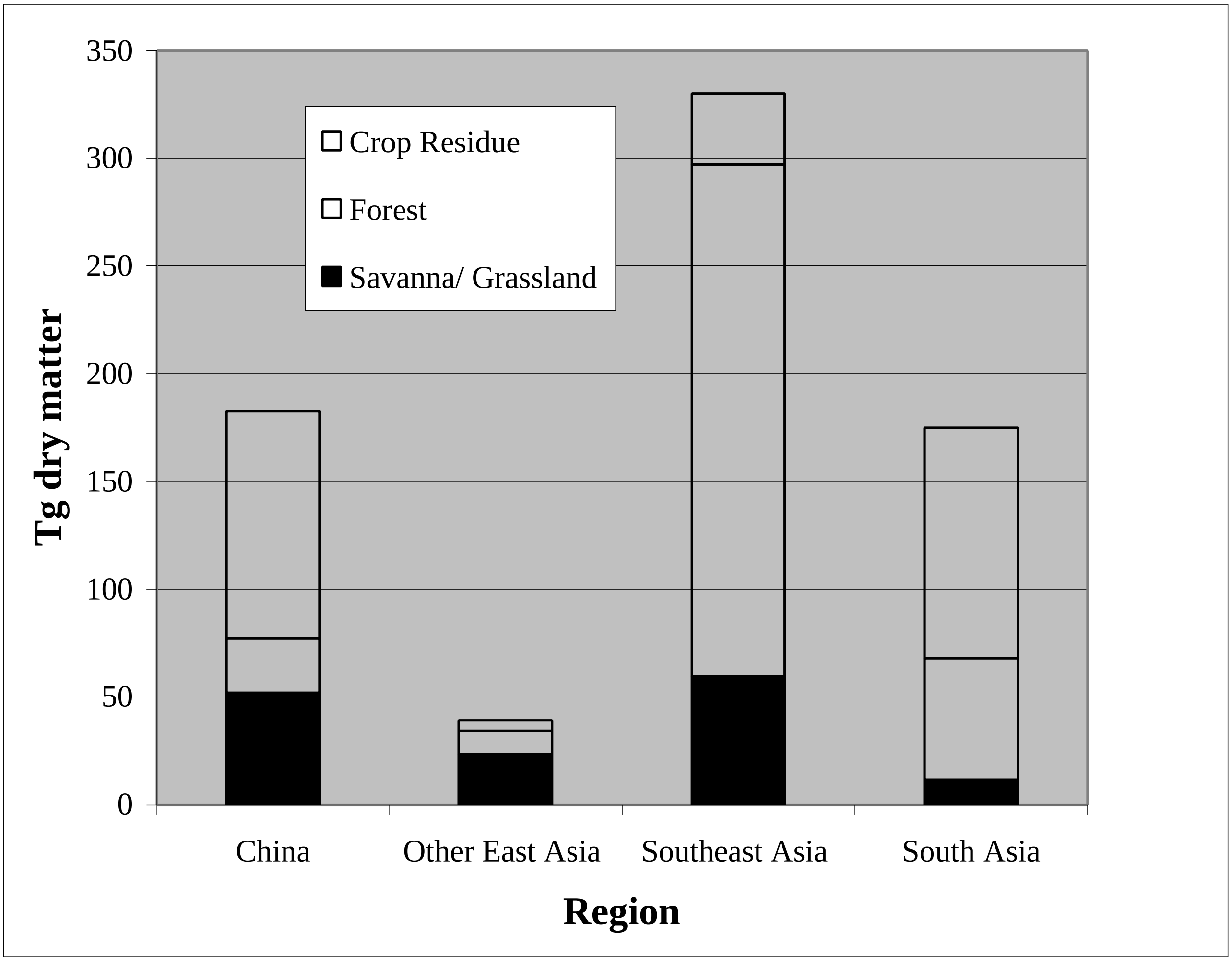
350
300
250
200
150
100
50
0
Tg dry matter
Crop Residue
Forest
Savanna/ Grassland
China
Other East Asia
Southeast Asia
South Asia
Region

**Figure 2.**

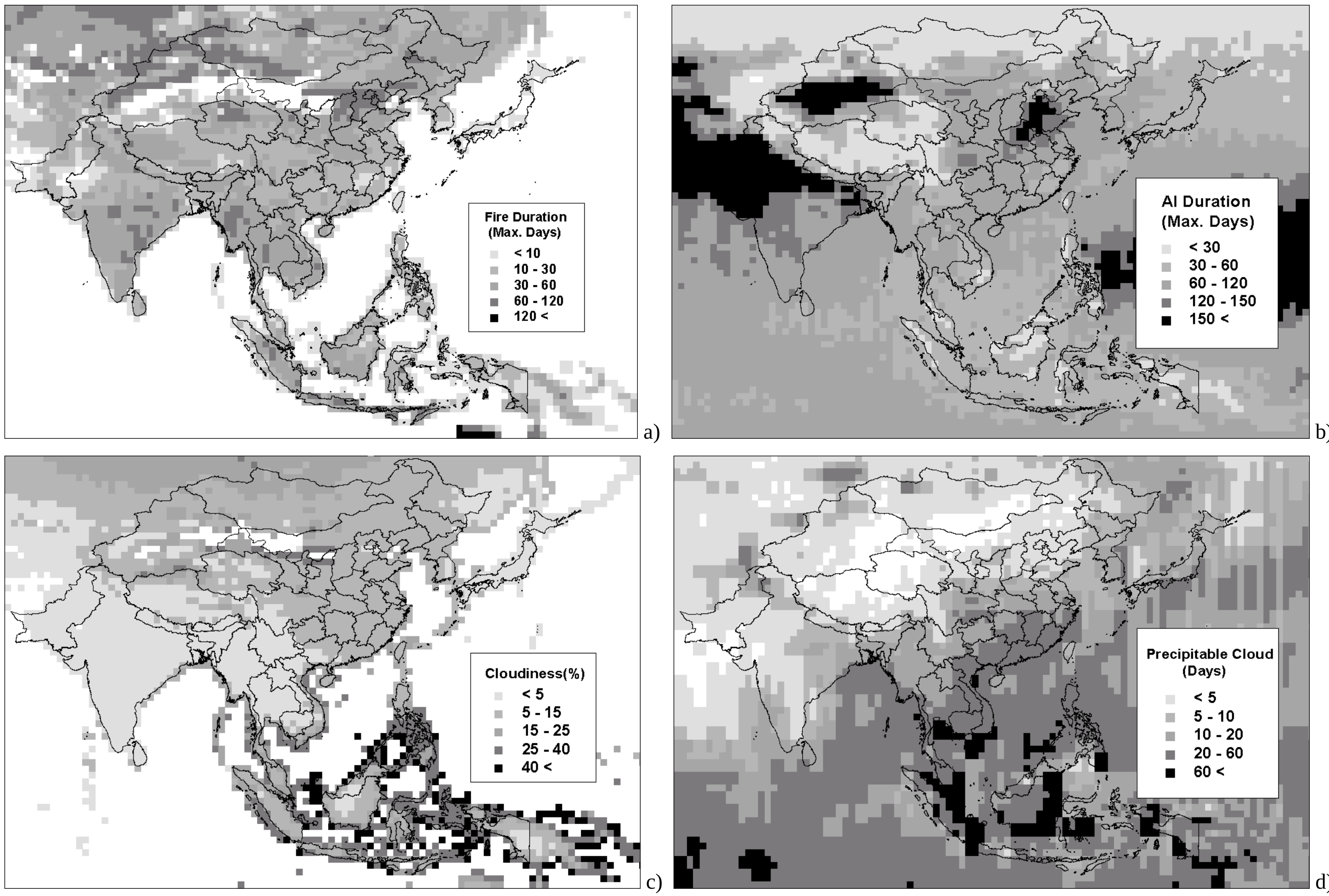
Fire Duration
(Max. Days)
< 10
10 - 30
30 - 60
60 - 120
120 <
a)
AI Duration
(Max. Days)
< 30
30 - 60
60 - 120
120 - 150
150 <
b)
Cloudiness(%)
< 5
5 - 15
15 - 25
25 - 40
40 <
c)
Precipitable Cloud
(Days)
< 5
5 - 10
10 - 20
20 - 60
60 <
d)

**Figure 3.**

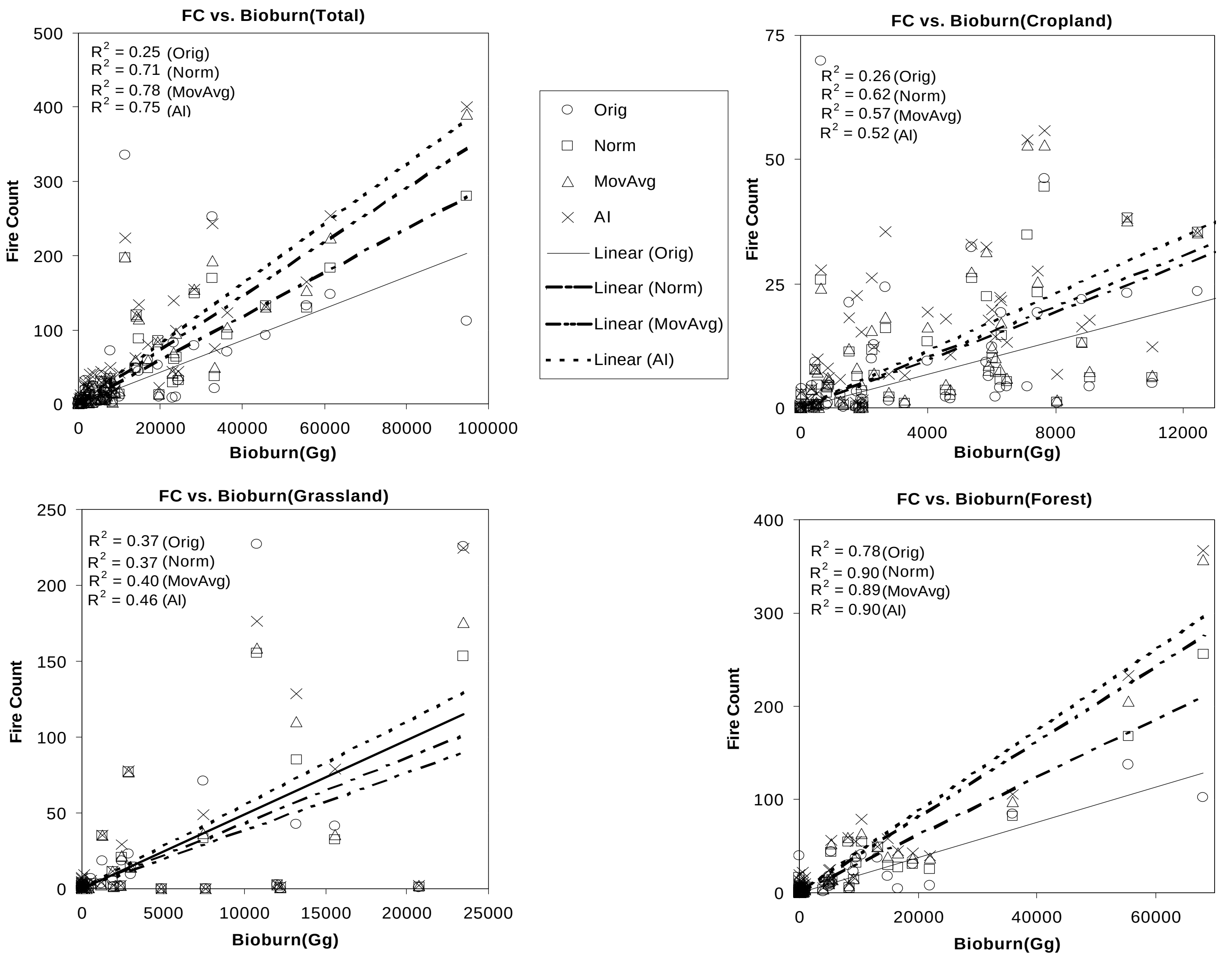

FC vs. Bioburn(Total)
R² = 0.25 (Orig)
R² = 0.71 (Norm)
R² = 0.78 (MovAvg)
R² = 0.75 (AI)
Fire Count
Bioburn(Gg)
0
100
200
300
400
500
0
20000
40000
60000
80000
100000
Orig
Norm
MovAvg
AI
Linear (Orig)
Linear (Norm)
Linear (MovAvg)
Linear (AI)
FC vs. Bioburn(Cropland)
R² = 0.26 (Orig)
R² = 0.62 (Norm)
R² = 0.57 (MovAvg)
R² = 0.52 (AI)
Fire Count
Bioburn(Gg)
0
25
50
75
0
4000
8000
12000
FC vs. Bioburn(Grassland)
R² = 0.37 (Orig)
R² = 0.37 (Norm)
R² = 0.40 (MovAvg)
R² = 0.46 (AI)
Fire Count
Bioburn(Gg)
0
50
100
150
200
250
0
5000
10000
15000
20000
25000
FC vs. Bioburn(Forest)
R² = 0.78 (Orig)
R² = 0.90 (Norm)
R² = 0.89 (MovAvg)
R² = 0.90 (AI)
Fire Count
Bioburn(Gg)
0
100
200
300
400
0
20000
40000
60000


**Figure 4.**

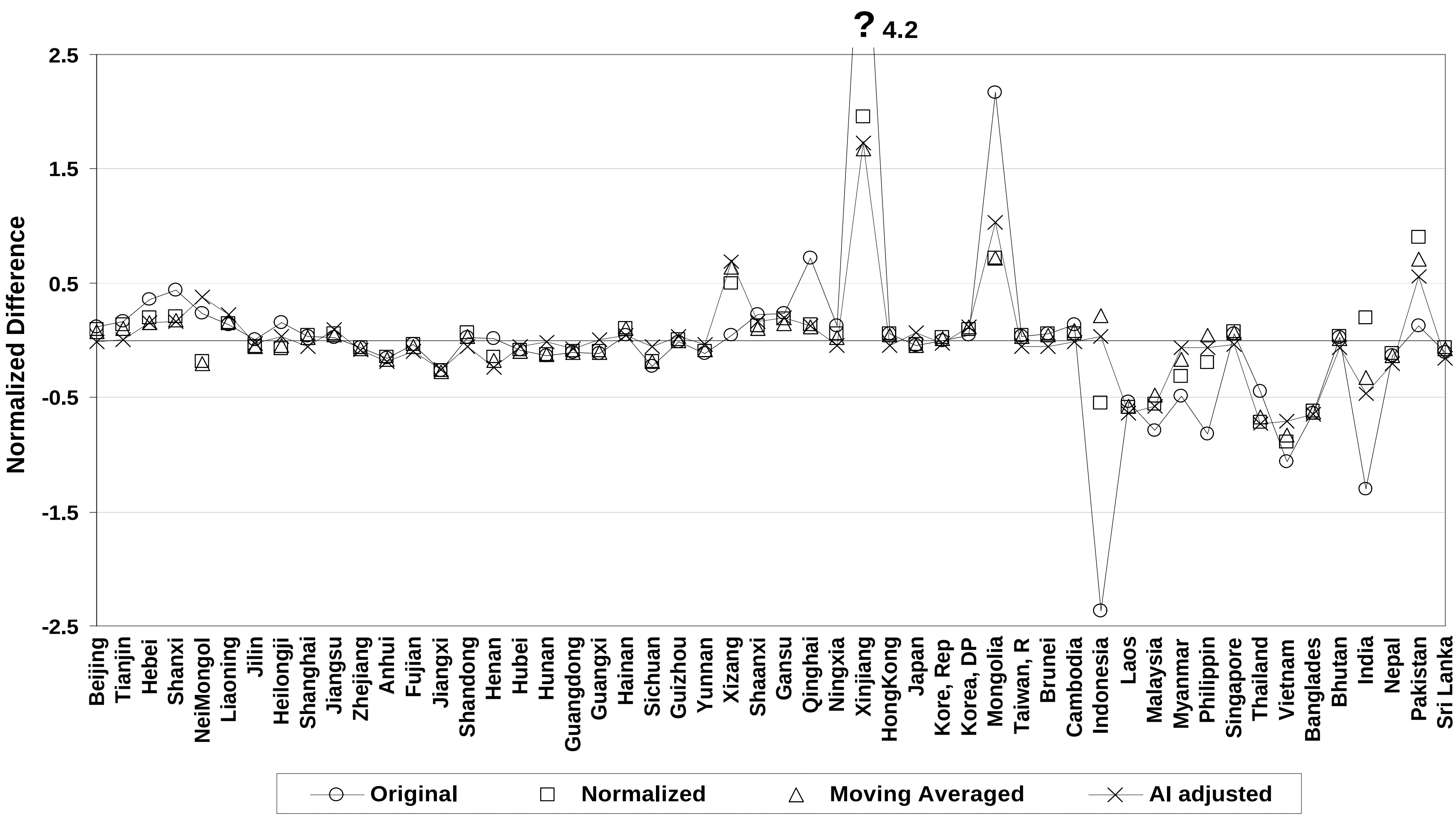
? 4.2
2.5
1.5
0.5
-0.5
-1.5
-2.5
Normalized Difference
Beijing
Tianjin
Hebei
Shanxi
NeiMongol
Liaoning
Jilin
Heilongji
Shanghai
Jiangsu
Zhejiang
Anhui
Fujian
Jiangxi
Shandong
Henan
Hubei
Hunan
Guangdong
Guangxi
Hainan
Sichuan
Guizhou
Yunnan
Xizang
Shaanxi
Gansu
Qinghai
Ningxia
Xinjiang
HongKong
Japan
Kore, Rep
Korea, DP
Mongolia
Taiwan, R
Brunei
Cambodia
Indonesia
Laos
Malaysia
Myanmar
Philippin
Singapore
Thailand
Vietnam
Banglades
Bhutan
India
Nepal
Pakistan
Sri Lanka
Original
Normalized
Moving Averaged
AI adjusted

**Figure 5.**

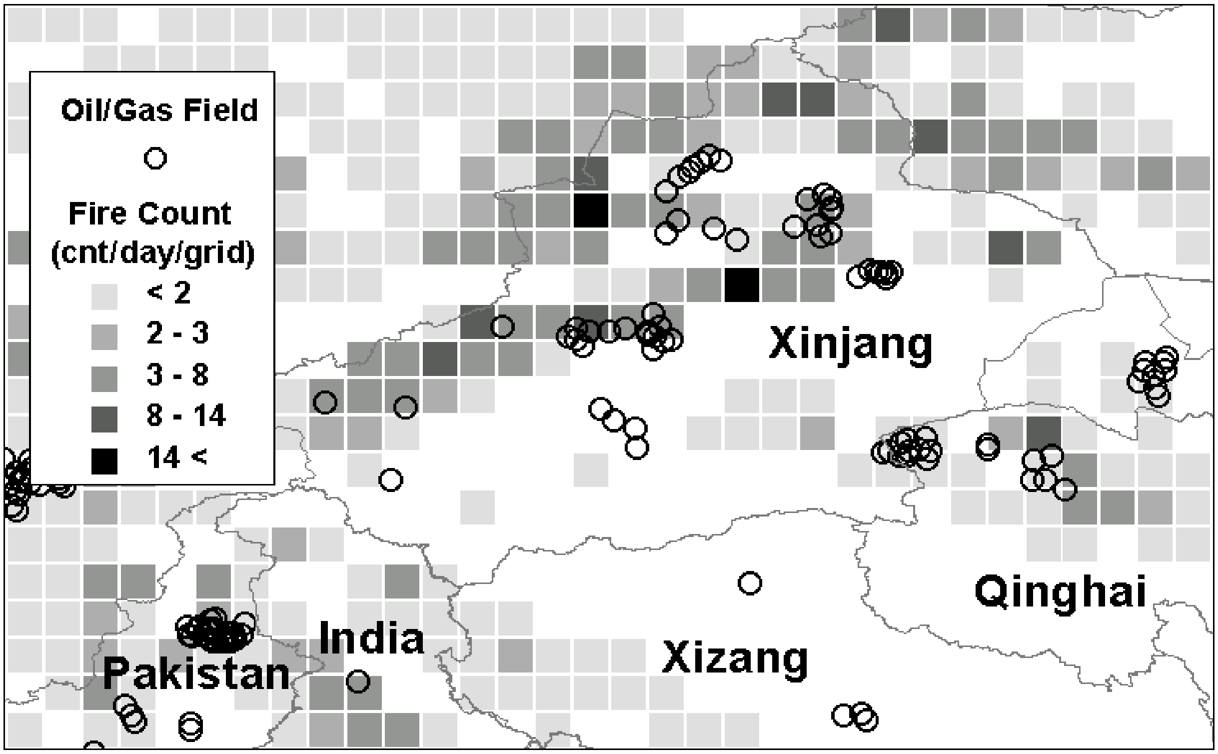
Oil/Gas Field
Fire Count
(cnt/day/grid)
< 2
2 - 3
3 - 8
8 - 14
14 <
Xinjang
Qinghai
Xizang
India
Pakistan

**Figure 6.**

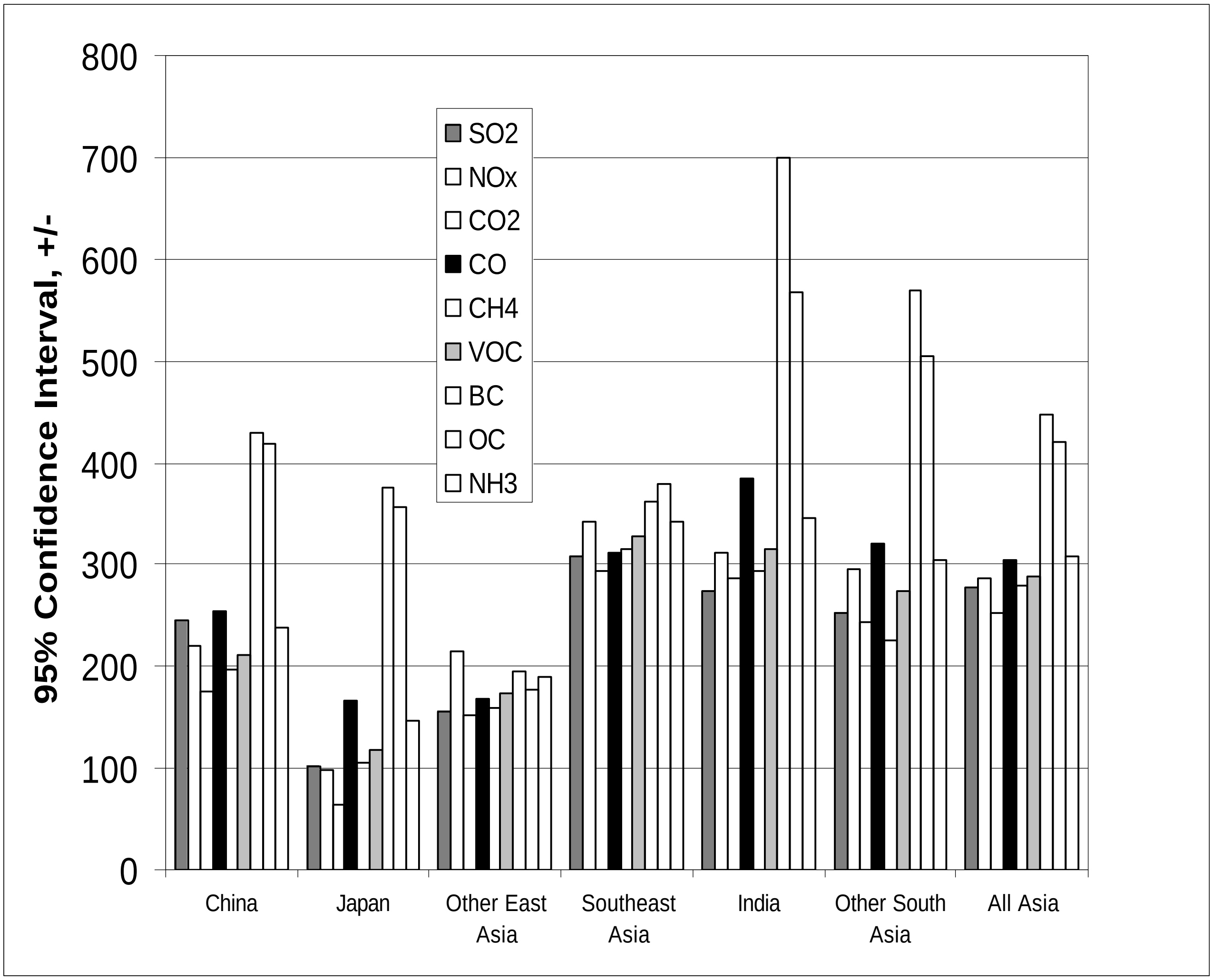
800
700
600
500
400
300
200
100
0
95% Confidence Interval, +/-
SO2
NOx
CO2
CO
CH4
VOC
BC
OC
NH3
China
Japan
Other East Asia
Southeast Asia
India
Other South Asia
All Asia

**Figure 7.**

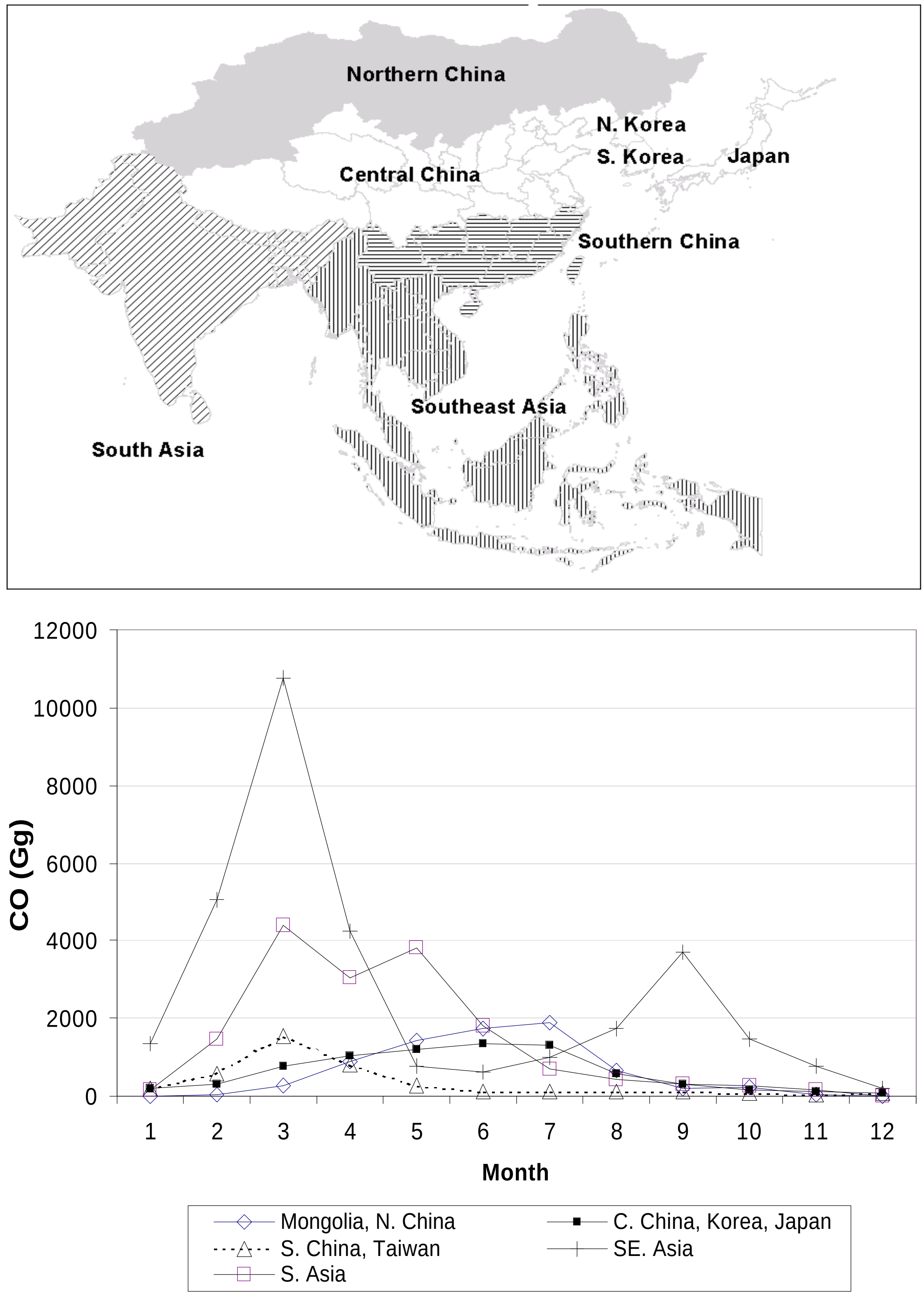

Northern China
N. Korea
S. Korea
Japan
Central China
Southern China
Southeast Asia
South Asia
12000
10000
8000
6000
4000
2000
0
CO (Gg)
1
2
3
4
5
6
7
8
9
10
11
12
Month
Mongolia, N. China
C. China, Korea, Japan
S. China, Taiwan
SE. Asia
S. Asia


**Figure 8.**

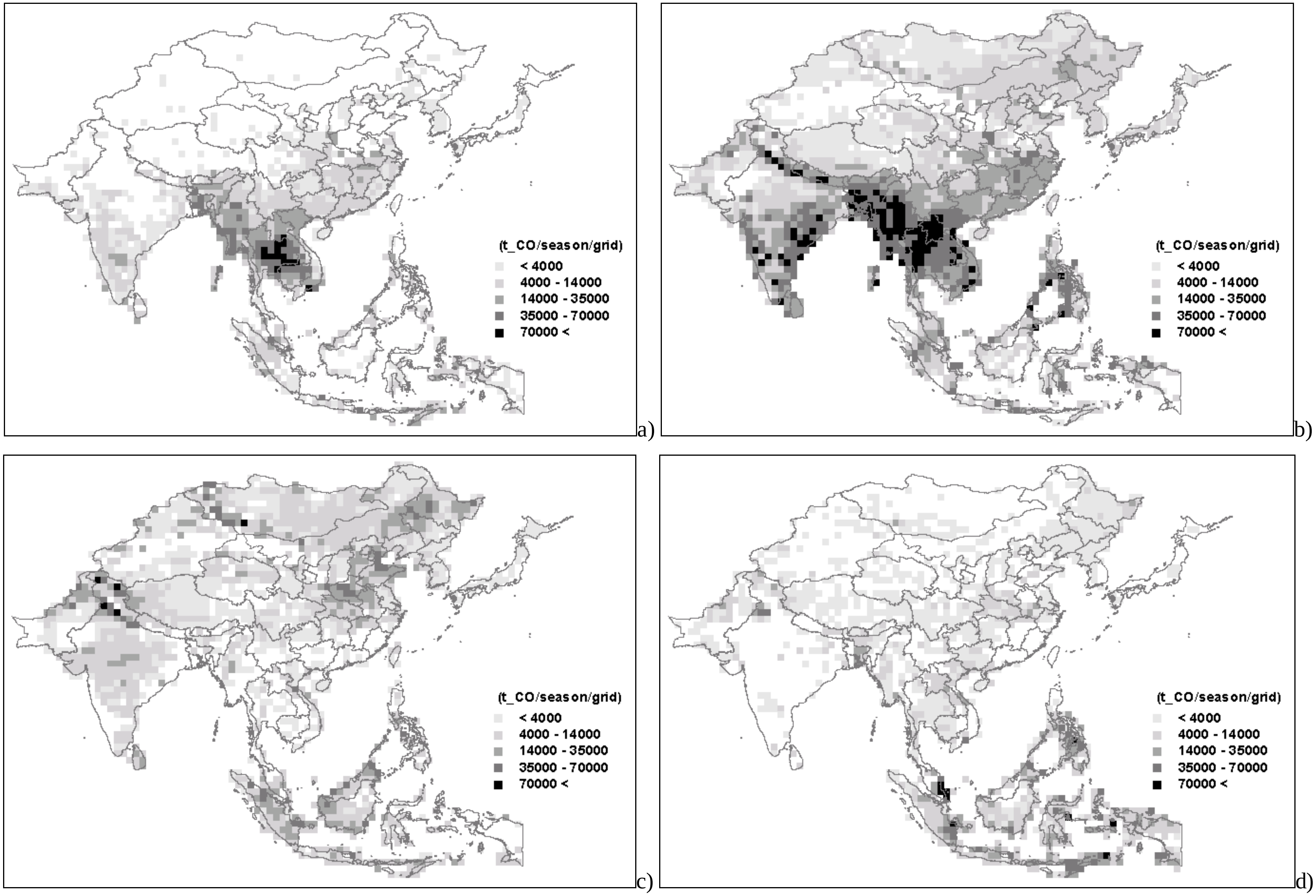
(t_CO/season/grid)
< 4000
4000 - 14000
14000 - 35000
35000 - 70000
70000 <
a)
(t_CO/season/grid)
< 4000
4000 - 14000
14000 - 35000
35000 - 70000
70000 <
b)
(t_CO/season/grid)
< 4000
4000 - 14000
14000 - 35000
35000 - 70000
70000 <
c)
(t_CO/season/grid)
< 4000
4000 - 14000
14000 - 35000
35000 - 70000
70000 <
d)

**Figure 9.**

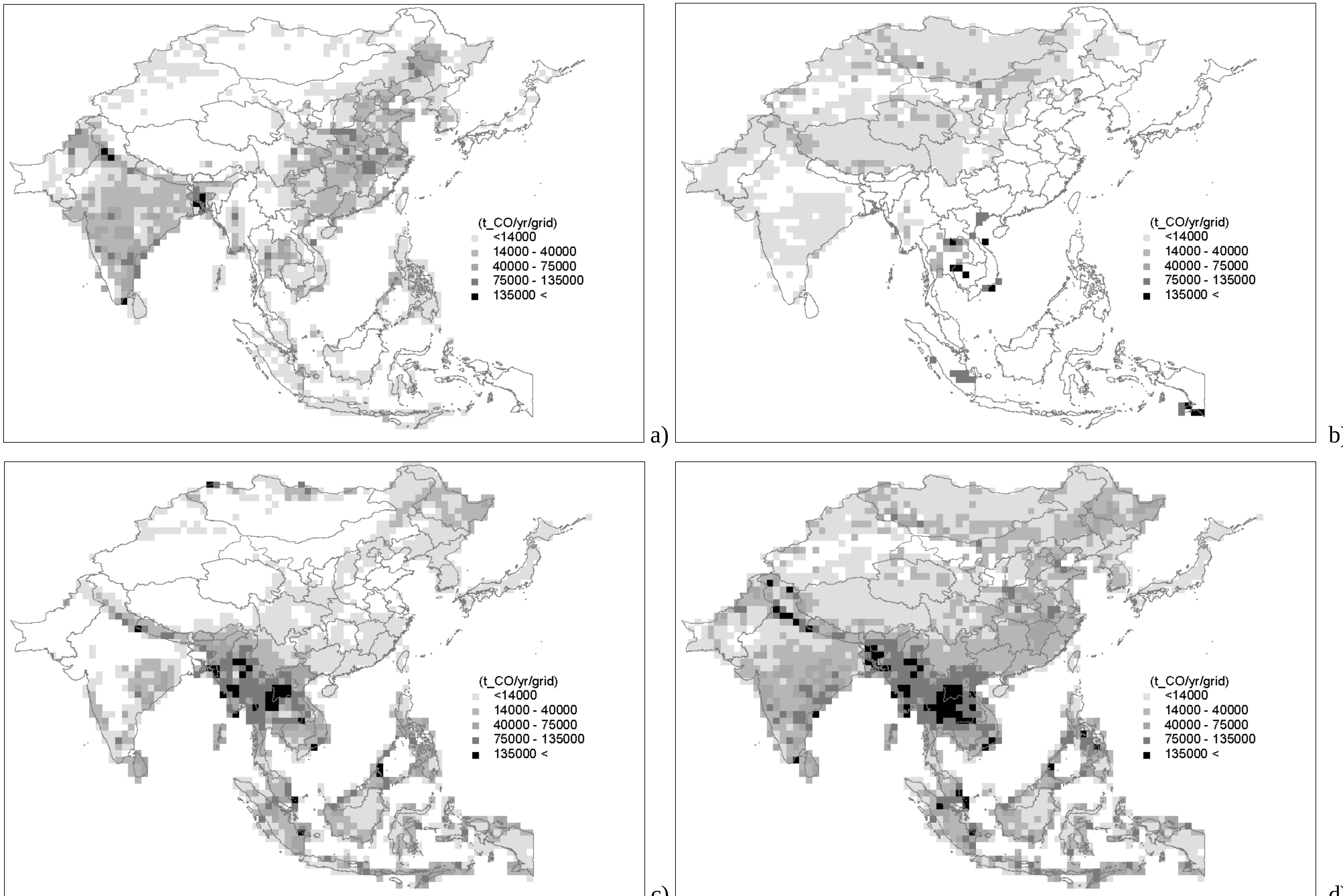
(t_CO/yr/grid)
<14000
14000 - 40000
40000 - 75000
75000 - 135000
135000 <
a)
b)
c)
d)

**Figure 10.**

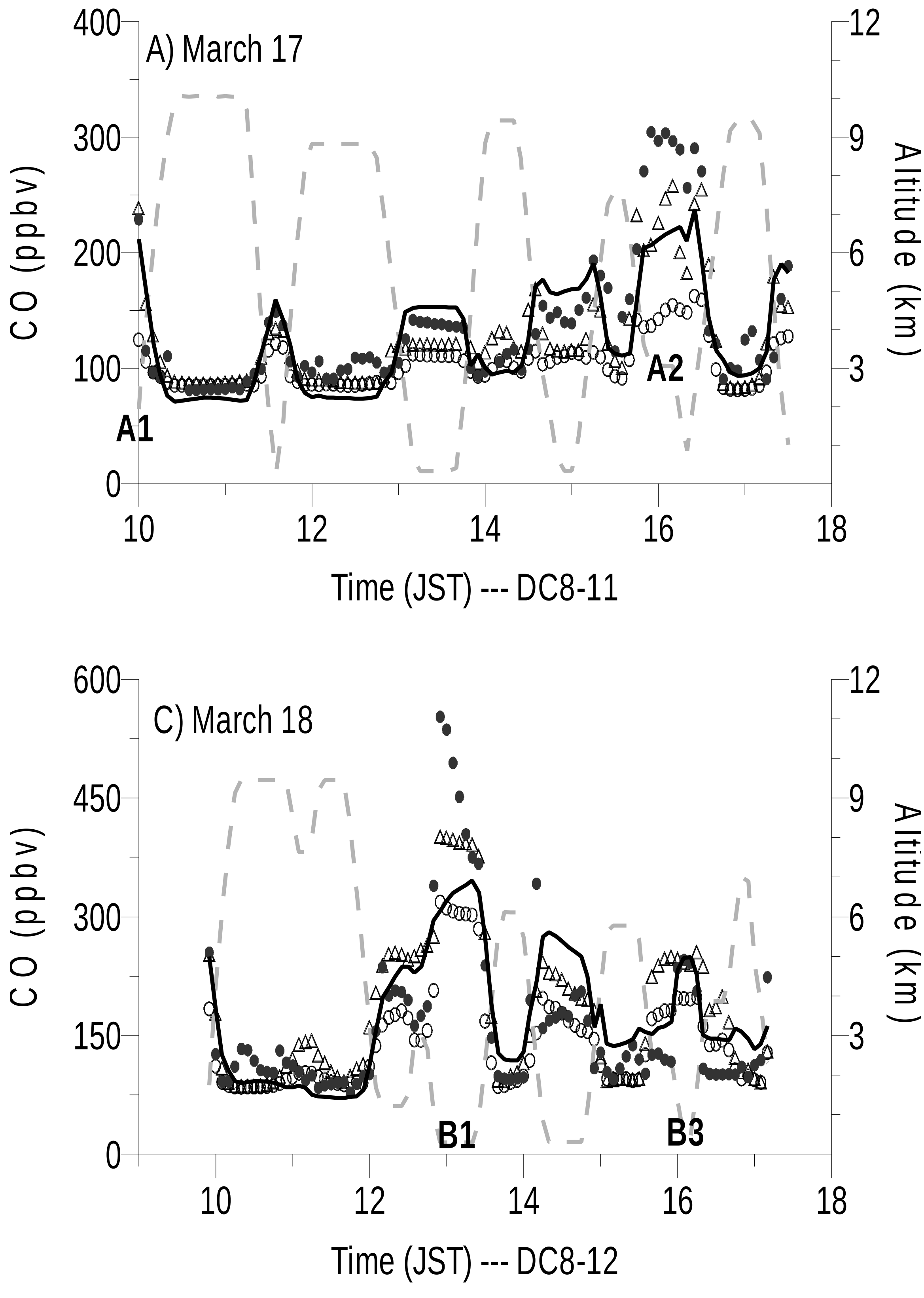
A) March 17
CO (ppbv)
Altitude (km)
A1
A2
Time (JST) --- DC8-11
C) March 18
B1
B3
Time (JST) --- DC8-12

**Figure 11.**